JUNE, 2014 M.Sc. in Electrical and Electronics Engineering Ali A. H. KARAH BASH

UNIVERSITY OF GAZİANTEP

GRADUATE SCHOOL OF

NATURAL & APPLIED SCIENCES

A COMPRESSIVE SENSING BASED ON WATERMARKING SCHEME FOR SPARSE IMAGE

M. Sc. THESIS

IN

ELECTRICAL AND ELECTRONICS ENGINEERING

BY

ALI A. H. KARAH BASH

JUNE 2014

a compressive sensing based on watermarking scheme for sparse image

M.Sc. Thesis

In

Electrical and Electronics Engineering

University of Gaziantep

Supervisor

Assist. Prof. Dr. Sema Koç KAYHAN

By

Ali A. H. KARAH BASH

june 2014

REPUBLIC OF TURKEY
UNIVERSITY OF GAZİANTEP
GRADUATE SCHOOL OF NATURAL & APPLIED SCIENCES
ELECTRICAL AND ELECTRONIC ENGINEERING
DEPARTMENT

Name of the thesis: A Compressive Sensing Based on Watermarking Scheme for Sparse Image.

Name of the student: Ali A. H. KARAH BASH

Exam date:02/06/2014

Approval of the Graduate School of Natural and Applied Sciences

Assoc. Prof. Dr. Metin BEDİR

Director

I certify that this thesis satisfies all the requirements as a thesis for the degree of Master of Science.

Prof. Dr. Ergun ERÇELEBİ

Head of Department

This is to certify that we have read this thesis and that in our consensus/majority opinion it is fully adequate, in scope and quality, as a thesis for the degree of Master of Science.

Assist. Prof. Dr. Sema Koç KAYHAN

Supervisor

Examining Committee Members	Signature
Prof. Dr. Ergun ERÇELEBI	.....
Assist. Prof. Dr. Ahmet Hanifi ERTAŞ	.....
Assist. Prof. Dr. Sema Koç KAYHAN	.....

I hereby declare that all information in this document has been obtained and presented in accordance with academic rules and ethical conduct. I also declare that, as required by these rules and conduct, I have fully cited and referenced all material and results that are not original to this work.

Ali A. H. KARAH BASH

ABSTRACT

A COMPRESSIVE SENSING BASED ON WATERMARKING SCHEME FOR SPARSE IMAGE

Ali A. H. KARAH BASH
M.Sc. Thesis in Electrical and Electronics Eng.
Supervisor: Assist. Prof. Dr. Sema Koç KAYHAN
June 2014
85 pages

The traditional Nyquist Shannon theorem explains that the number of samples which are needed for recovering a signal must be at least twice the maximum frequency in the bandwidth of a signal. This approach is used in all applications of the signal processing. This problem is solved by using a new sampling method developed called Compressive Sampling or Compressive Sensing (CS), where it is used to recover signals or images from far fewer measurements or samples than the traditional theorem. CS theory depends on Sparsity principle, thereby the signals or images must be sparse. However, most of the natural signals or images are not sparse. Therefore, there are some transformation methods used to alter these signals or images into sparse like Discrete Cosine Transform (DCT), Discrete Wavelet Transform (DWT) and Discrete Fourier Transform (DFT).

In this thesis, we integrate the watermarking technology and compressive sensing theory to protect the watermarking image in the compressive sensing measurements. The watermarking image is embedded into the compressive measurement vectors. The measurement vectors are sparse in a suitable basis. The resulting watermarked measurements recover by using both the Orthogonal Matching Pursuit (OMP) and Orthogonal Matching Pursuit With Partially Known Support (OMP-PKS) reconstruction algorithms. Then the decoder procedure utilizes to extract the watermarking image. In experimental study, the results obtained by comparing between the OMP and OMP-PKS algorithms to clarify the performance of them. The results show that the OMP-PKS algorithm achieves performance superior to that of the OMP reconstruction algorithm.

Key Words: Watermarking image, CS, OMP and OMP-PKS algorithms.

ÖZET

SEYREK İMGELERİN SIKIŞTIRMALI ÖRNEKLEME YÖNTEMİ İLE DAMGALANMASI

Ali A. H. KARAH BASH
Yüksek Lisans Tezi, Elektrik-Elektronik Müh. Bölümü
Tez Yöneticisi: Yrd. Doç. Dr. Sema Koç KAYHAN
Haziran 2014
85 sayfa

Nyquist Shannon teorimine göre bir işaretin geri kazanımı için örnekleme sayısı en az işaretin maksimum frekansının iki katı olmalıdır. İşaret ile ilgili pek çok alanda bu yaklaşım kullanılmaktadır. Bu yaklaşımda çok fazla örnek kullanılmaktadır. Örnekleme sayısını azaltmak için sıkıştırmalı örnrkleme algoritmaları (CS) geliştirilmiştir. Bu algoritma ile çok az sayıda örnek kullanarak sinyalin geri kazanımı mümkün olmaktadır. CS teorisi seyreklik prensibine dayandığı için örneklenecek olan işaretin veya imgenin de seyrek olması gerekir.

Fakat pek çok doğal imge veya işaret seyrek yapıda değildir. Bu nedenle bu sinyalleri seyrek olarak ifade edebilmek için Ayrık Kosinüs Dönüşümü (DCT), Fourier Dönüşümü (DFT) veya Dalgacık Dönüşümü (DWT) gibi dönüşüm methodları kullanılmaktadır. Sıkıştırmalı örnekleme ve işaretin geri kazanımı sırasında bağımsız ölçüm matrisi kullanılmaktadır..

Bu tezde, sıkıştırmalı örnekleme ölçümlerindeki damgalama imgesini korumak için CS tabanlı bir damgalama algoritması geliştirilmiştir. Öncelikle damgalama imgesi CS vektörlerine gömülür. Örnekleme vektörünün de seyreltilmiş olması gerekmektedir. Sonuçta elde edilen damgalama ölçümleri farklı dik eşleştirme algoritmaları ((Orthogonal Matching Pursuit, OMP), (Orthogonal matching pursuit with partially known support OMP-PKS)) kullanılarak geri kazanılmaktadır. Damgalama imgesini çıkarmak için kod çözme algoritması kullanılmaktadır.

Deneysel çalışmalarda OMP ve OMP-PKS algoritmalarının sonucu karşılaştırılmış ve OMP-PKS algoritmasının OMP ye göre daha iyi sonuç verdiği görülmüştür.

Anahtar Kelimeler: Damgalama imgesi, CS, OMP ve OMP-PKS algoritmaları.

To My Parents

ACKNOWLEDGMENTS

I thank Allah who helped and guided me to complete this work. Also, I would like to express my deep thankfulness and sincere gratitude to my advisor Assist. Prof. Dr. Sema Koç Kayhan for her direction, suggestion and encouragement. This work would not be possible without her precious support and advice.

I would like to thank the government of Turkey represented by Ministry of Turks Abroad and Related Communities (Yurtdışı Türkler ve Akraba Topluluklar Bakanlığı) for granting me the scholarship to study in the Turkey and supporting me financially during my study in Gaziantep University.

In addition, I present a private thanks to my parents for encouraging and supporting me in this work and throughout my study. It is my pleasure to thank the people who supported me to make this thesis possible. I would also like to thank my friend Hasan Alpegamberli for his support and help throughout this work. I would like to thank Mr. Taha Al-Meryem, who introduced me into the field of Linear algebra and gave me a lot of guidance and teaching.

TABLE OF CONTENTS

Page

ABSTRACT V
ÖZET VI
ACKNOWLEDGMENTS VIII
CONTENTS IX
LIST OF TABLES X
LIST OF FIGURES XI
LIST OF SYMBOLS XIV
LIST OF ABBREVIATIONS XV
CHAPTER 1: INTRODUCTION I
CHAPTER 2: OVERVIEW 8
2.1 Compressive Sensing CS 8
2.1.1 Overview of Compressive Sensing CS 8
2.1.2 Applications of CS 11
2.2 Overview of Reconstruction Algorithms 15
2.2.1 L1 minimization algorithm 15
2.2.2 Orthogonal matching pursuit OMP 17
2.2.3 Orthogonal matching pursuit with partially known support OMP-PKS 22
2.3 Watermarking image 25
2.3.1 Overview of Watermarking Image 25
2.3.2 Watermarking properties 26
2.3.3 Application of the digital watermarking 27
CHAPTER 3: METHODOLOGY 30
3.1 Compressive Sensing CS 30
3.2 The reconstruction algorithms 33
3.2.1 L1 minimization algorithm 33
3.2.2 Orthogonal matching pursuit OMP 33
3.2.3 Orthogonal matching pursuit with partially known support OMP-PKS 34
3.3 Digital Watermarking 37
3.3.1 The encoder algorithm 38
3.3.2 The reconstruction algorithms 39
3.3.3 The decoder algorithm 40
3.4 Proposed Flowchart 44
CHAPTER 4: RESULTS AND DISCUSSION 47
CHAPTER 5: CONCLUSION AND SUGGESTIONS FOR FUTURE WORKS 61
REFERENCES 62

LIST OF TABLES

Page

Table 2.1. Orthogonal Matching Pursuit OMP algorithm. 18

Table 2.2. Orthogonal Matching Pursuit with partially known support OMP-PKS algorithm. 24

Table 3.1. OMP-PKS and OMP algorithms in the first decoder method.....41

Table 3.2. OMP-PKS and OMP algorithms in the second decoder method 43

Table 4.1. PSNR and its execution time with different measurement rates *M/N* by using the three reconstruction algorithms with the first and second decoder methods....59

Table 4.2. PSNR and its execution time with different Sparsity rates *K/N* by using the three reconstruction algorithms with the first and second decoder methods. 60

LIST OF FIGURES

Page

Figure 1.1. Basic block diagram of CS technique. 2

Figure 1.2. Traditional data acquisition approach [3]. 3

Figure 1.3. CS data acquisition approach [3]. 3

Figure 1.4. A scheme of the general watermarking encoder and decoder. 7

Figure 1.5. A scheme of CS watermarking procedure. 7

Figure 2.1. Block diagram of Compressive Imaging Camera [22]. 12

Figure 3.1. Compressive acquisition and reconstruction [80]..... 32

Figure 3.2. Wavelet decomposition by filter bank analysis. HP and LP are high pass filter and low pass filter, respectively [64]..... 35

Figure 3.3. The octave-tree discrete wavelet transform: (a) the original image and (b) the wavelet transformed image. Sub-bands inside the blue, green and red windows are the first, the second and the third level sub-bands, respectively [65]. 35

Figure 3.4. Wavelet transform and its block processing: (a) wavelet transformed image, (b) wavelet sub-bands rearranging and (c) wavelet blocks [65]. 36

Figure 3.5. The coefficients of LL3 sub-band, that are in the first four columns at the red region.....37

Figure 3.6. Watermarking image embedding structure [10].....38

Figure 3.7. The proposed flowchart.....46

Figure 4.1. (a) Original Lena image and (b) Watermarking image.....47

Figure 4.2. (a) Random Gaussian distribution of the sensing matrix Φ. (b) Random Gaussian distribution of ΦQ matrices.....48

Figure 4.3. The quality of the reconstructed image with the extracted watermarking image in varying *M/N* rates using L1-min in the first decoder method.....49

Figure 4.4. The quality of the reconstructed image with the extracted watermarking image in varying *M/N* rates using L1-min in the second decoder method.....49

Figure 4.5. The quality of the reconstructed image with the extracted watermarking image in varying *M/N* rates using the OMP algorithm in the first decoder method.....50

Figure 4.6. The quality of the reconstructed image with the extracted watermarking image in varying *M/N* rates using the OMP algorithm in the second decoder method.....50

Figure 4.7. The quality of the reconstructed image with the extracted watermarking image in varying M/N rates using the OMP-PKS algorithm in the first decoder method.....51

Figure 4.8. The quality of the reconstructed image with the extracted watermarking image in varying *M/N* rates using the OMP-PKS algorithm in the second decoder method. 51

Figure 4.9. (a) Residual values with different *M/N* in the first decoder method.....52

Figure 4.9. (b) Residual values with varying *M/N* in the second decoder method. (c) MSE values with varying *M/N* in the first decoder method. 53

Figure 4.9. (d) MSE values with different *M/N* in the second decoder method. (e) PSNR values with varying *M/N* in the first decoder method.....54

Figure 4.9. (f) PSNR values with different *M/N* in second decoder method. 55

Figure 4.10. Performance of the L1-min, OMP and OMP-PKS algorithms in varying *K/N* values, (a) Residual with different *K/N* values in the first decoder method. (b) Residual with different *K/N* values in the second decoder method.....56

Figure 4.10. Performance of the L1-min, OMP and OMP-PKS algorithms in varying *K/N* values, (c) MSE with different *K/N* values in the first decoder method. (d) MSE with different *K/N* values in the second decoder method.....57

Figure 4.10. Performance of the L1-min, OMP and OMP-PKS algorithms in varying *K/N* values, (e) PSNR with different *K/N* values in the first decoder method. (f) PSNR with different *K/N* values in the second decoder method. …….58

LIST OF SYMBOLS

x	Signal or image which is usually sparse or compressible.
y	Observation or Measurement vector.
R	Real numbers space.
N	Rows of the vector x.
M	Rows of the measurement vector y.
K	Sparsity (number of nonzero entries of the vector x).
Φ	Projection or sensing matrix of size $M \times N$.
Ψ	Spatial domain in size N x N.
φ_i	ith column of the matrix Φ.
I	Active set.
I_c	Inactive set.
t	Iteration counter.
r	Residual vector at iteration t.
δ	Restricted Isometry Constant.
μ	Incoherence between two columns of the measurement matrix Φ.
f_i	Transform Domain components.
V	Watermarking image.
y_v	Watermarked compressive sensed measurement.
L	Number of bits in the watermarking image.
D	Random matrix by M x L.
$\hat{Z}$	Measurement vector combines x and V.
H	Measurement matrix combines Φ and D.
T	Index of known support part of a sparse image.
Q	Random matrix with M x N.

LIST OF ABBREVIATIONS

CS	Compressed Sensing.
L1-min	L1 minimization algorithm.
OMP	Orthogonal Matching Pursuit.
MP	Matching pursuit**.**
OMP-PKS	Orthogonal Matching Pursuit with partially known support.
LP	Linear programing.
BP	Basis pursuit.
TOMP	Tree based Orthogonal matching pursuit.
RIP	Restricted Isometry Property.
UUP	Uniform uncertainty principle.
NP	Nondeterministic polynomial time.
SBS	Sequential basis selection.
FSR	Forward Stepwise Regression.
CMP	Complementary Matching Pursuit.
OCMP	Orthogonal Complementary Matching Pursuit.
GOMP	Generalized Orthogonal Matching Pursuit.
STOMP	Stage-Wise Orthogonal Matching Pursuit.
ROMP	Regularized Orthogonal Matching Pursuit.
MR	Magnetic Resonance.
DWT	Discrete Wavelet Transform.
TV min	Total Variation Minimization.
DCT	Discrete Cosine Transform.
DFT	Discrete Fourier Transform.
SPC	Single Pixel Camera.

DMD	Digital Micro mirror Device.
CRSI	Curvelet Based Recovery By Sparsity Promoting Inversion.
GPRs	Ground Penetrating Radars.
AIC	Analog to Information Conversion.
ADC	Analog to Digital Converter.
DIVX	Digital Video Disk Players.
DVD	Digital Video Disks.
LARS	Least Angle Regression.
LASSO	Least Absolute Shrinkage and Selection Operator.
PSNR	Peak Signal to Noise Ratio.
MSE	Mean Square Error.

CHAPTER 1

INTRODUCTION

Data transmission in the signal processing field is often executed in the digital domain, because this process occupies lower bandwidth compared to the analog domain. So the analog to digital converter is used for converting the band limited signal to a digital signal to implement the sampling operation at a particular sampling rate. The uniformly spaced samples result from sampling the signal. These uniformly spaced samples are used for recovering the signal back to the origin by the Nyquist Shannon theorem. The condition of the Nyquist Shannon theorem in the signal recovering case is that the number of samples must be at least twice the maximum frequency of the interested signal, i.e. the perfect recovery encloses when the sampling rate is twice the maximum frequency of the original signal. The resulting particular rate and sampling the signal are called Nyquist rate.

Regrettably, in the signal processing applications field, there are far too many samples when using the Nyquist Shannon theorem in the data sampling. Therefore, the amount of data at the transmitter increases, which in turn leads to increased cost of the building devices that are able to acquire the samples at the Nyquist rate. The data compression is the best method to cope this problem. Data compression finds a brief representation of a signal that is capable of reaching the target rate with a reasonable distortion. The transform coding is a known technique used in the data compression, which is dependent on a basis that supplies sparse approximation of the signal.

The disadvantage of the transform coding technique is sampling the data at Nyquist rate before compressing it; this increases cost of acquiring the sampled devices at Nyquist rate. To cope this case, there is a new technique developed known Compressive Sampling or Compressive Sensing CS [1]. The CS technique is used to recover the original signal from far too few samples or measurements which lead to decrease cost

of acquiring the sampled devices [2]. Figure 1.1 shows the basic block diagram of CS technique, which $x \in R^N$ is the input signal with N length and $y \in R^M$ represents an M measurement vector; this has been arrived at by computing the correlation between x and measurement or projection matrix $\Phi \in R^{MxN}$, mathematically y is given as follows:

$$y_i = \langle x, \Phi_i \rangle. \text{ Where } i = 1, 2 \ldots M. \quad (1.1)$$

where $M << N$ and $\hat{x} \in R^N$ is the recovered signal from M measurements. The compressive sensing immediately acquires the compressed signal samples at a lower sampling rate instead of first data sampling, which acquires the compressed signal samples at a higher rate, then the sampling of data compresses, i.e. the data compression and sensing are achieved together. The input signal x is sparse or sparse in Ψ domain, in this case:

$$y_i = \langle \Psi\alpha, \Phi_i \rangle. \text{ Where } i = 1, 2 \ldots M. \quad (1.2)$$

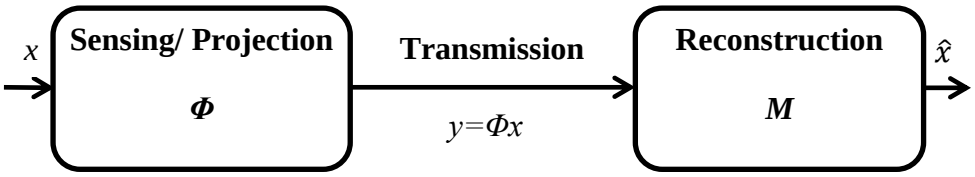

Figure 1.1. Basic block diagram of CS technique.

To perfectly recover the band limited signal by using the Nyquist Shannon theorem as depicted in Figure 1.2, a certain number of samples equal to the Nyquist rate are needed. When the sampling rate is less than the Nyquist rate, the original signal cannot be recovered by traditional recovery approaches. In contrast, in the compressive sensing as shown in Figure 1.3 though the samples are far too less than the samples that are needed in the conventional process, the original signal can be recovered.

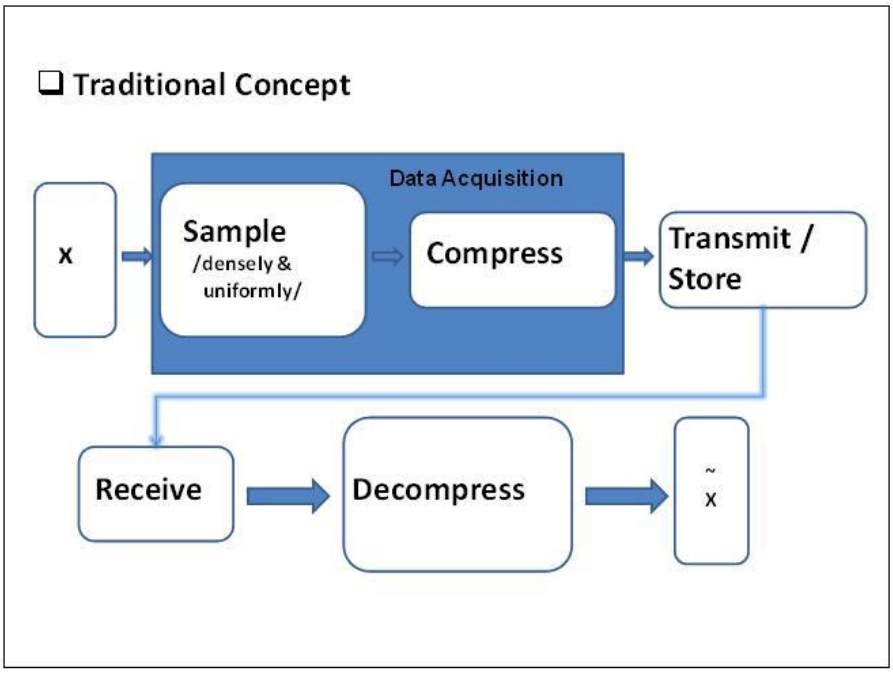

Figure 1.2. Traditional data acquisition approach [3].

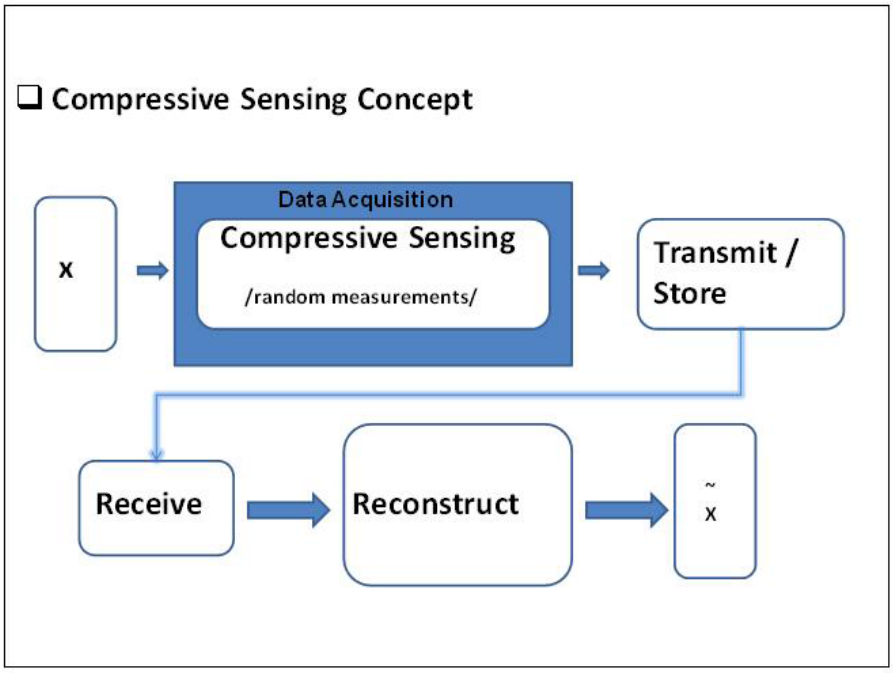

Figure 1.3. CS data acquisition approach [3].

The compressive sensing is different from the classical Nyquist paradigm which provides a sparse solution for underdetermined linear systems and is capable of recovering the signals from fewer samples than the Nyquist sampling rate. CS solves the problem of a limited number of samples that happens in different applications like data capturing devices and imaging techniques. In each case, CS provides a hopeful solution. The compressive sensing CS takes advantage of the Sparsity of signals in some transform domains and the incoherency of these measurements with the original domain is also taken.

In addition, CS deals with the compression and sampling in one step by computing the minimum samples. These samples have maximum information about the signal. Thus, the procedure described above minimizes the requirements to acquire and store a large number of samples because of their minimal values. There are many approaches that are reconstructed the sparse image like the optimization and the greedy methods. In this thesis, three reconstruction algorithms are explained, L1 minimization, orthogonal matching pursuit OMP and orthogonal matching pursuit with partially known support OMP-PKS, which are employed to reconstruct the measurement vectors resulting from the CS.

L1 minimization L1-min is one of the most famous reconstruction methods, which is used in the signal processing and optimization communities in the last years or so. L1-min is an efficient approach utilized in the CS theory, which reconstructs the sparse solution to a certain underdetermined linear equation system [1]. Let $x \in R^N$ is an unknown signal, a measurement vector $y \in R^M$ is generated by using the linear projection of y, where $y = \Phi x$, if the sensing matrix Φ is a full rank and over complete, i.e., $M \ll N$, an L1-min algorithm solves the following convex optimization problem:

$$\text{(F1): min } \|x\|_{l_1} \text{ subject to } y = \Phi x. \qquad (1.3)$$

where F1 formula represents a linear inverse problem, y is the number of measurements and is smaller than the number of unknowns x. The CS approach displays x as efficient sparse and measurement matrix Φ as incoherent in basis under which x is sparse. This Sparsity property of F1 is shown in the major applications as image processing, data

compression, sensor, recent computer vision and networks. The formula of F1 represents a Linear Programing LP problem shown in the basis pursuit BP [4]. The OMP is an iterative greedy algorithm, which is used in the sparse signal or sparse image reconstruction. In each iteration, OMP selects columns from the measurement matrix Φ which has best correlation with the residual r of the signal. Then the OMP produces a new approximation signal by projecting the signals onto the selected columns of measurement matrix Φ. This approach extends for the trivial greedy algorithm, which is successful in an orthonormal system. Also the OMP algorithm is simple and has fast implementation [5].

Let S be an arbitrary K-sparse signal in R^N, $y \in R^M$ is a measurement vector, Φ is an $M \times N$ measurement matrix and N measurements of the signal are observed in an M-dimensional measurement vector $y = \Phi S$. The columns of the measurement matrix Φ are denoted as $\{\varphi_1, \ldots, \varphi_N\}$. As mentioned earlier, it is natural to think of signal recovery as a problem dual to sparse approximation. Since S has only K nonzero coefficients, the measurement vector $y = \Phi S$ represents a linear combination of K columns from Φ, and y has K non-zero coefficients over the measurement matrix Φ. This idea allows transporting the sparse results from approximation to signal recovery problem. In particular, sparse approximation approaches are used for signal reconstruction. To match the ideal signal S, it is required to compute which columns of Φ combine with the measurement vector y. The algorithm idea is to choose columns in a greedy fashion. In each iteration, the column of Φ is selected; this has the strongest correlation with the remaining part of y. Then we subtract off its contribution to y and iterate on the residual. After K iteration, the algorithm will have identified the correct set of columns.

The OMP-PKS is a greedy algorithm used for image reconstruction from the measurement vectors and it is developed from the traditional OMP algorithm [6]. OMP-PKS provides a priori information about the coefficients of the sparse signal, that some coefficients are more important than the others. These important coefficients are selected as non-zero coefficients. The characteristic of OMP-PKS is the same as OMP, where the requirement of restricted isometry property RIP is not severed as BP [7]. OMP-PKS needs low measurement rates in the signal recovery. The OMP-PKS is different from

Tree based Orthogonal matching pursuit TOMP, where in the OMP-PKS the next basis selection is not dependent on the previously selected bases. But in the TOMP, the basis selections are compared with and selected a next good group of the related atoms in wavelet tree [8]. In the OMP-PKS, the partially known support ideas are required to enhance a performance of the reconstruction. The partially known support PKS provides priori information about the selected columns of the measurement matrix Φ. The PKS modifies OMP-PKS algorithm initialization because the columns of Φ are contributed with the measurement vector y before staring the iteration.

In the digital management, illegal manner can easily be used in contents of multimedia. Therefore, the easy distribution of multimedia data on the Internet needs some protection techniques to protect these data from unauthorized use. The digital watermarking is used for protection of the digital images [9]. Digital Watermarking is a visible or invisible identification code which is always embedded in the host media. In any digital watermarking technique, there are two main components: watermark embedding and watermark detection. Digital watermarking provides the embedding process to insert the data known as watermark into the contents of a multimedia involving as text documents, images, audio or video streams. The watermark is detected later by using the extraction algorithms. Figure 1.4 shows the watermarking scheme which consists of three parts:

1-The watermark.

2-The encoder (insertion algorithm).

3-The decoder (extraction or detection algorithm).

In this thesis, the watermarking algorithm has been used to insert the watermarking image into the compressive sensed measurement vector y as shown in the Figure 1.5 [10]. The measurement vectors are sparse in suitable basis. The resulting watermarked compressive sensed measurements are recovered by using the three reconstruction algorithms L1-min, OMP and OMP-PKS. Then the extraction algorithm is used to extract the watermarking image.

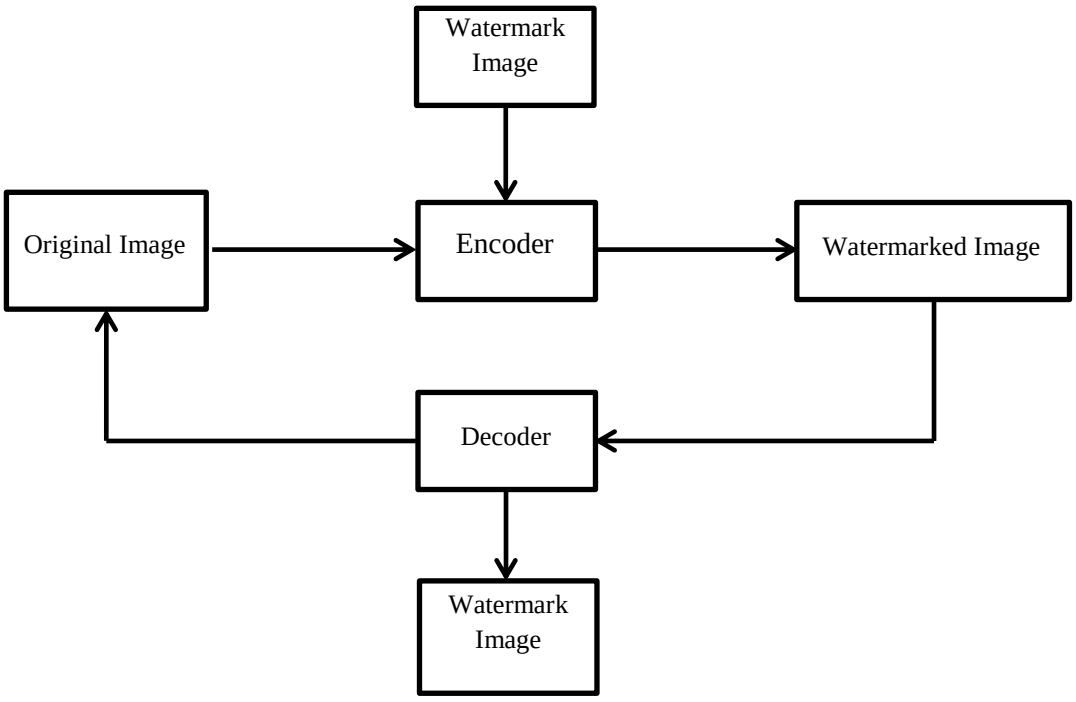

Figure 1.4. A scheme of the general watermarking encoder and decoder.

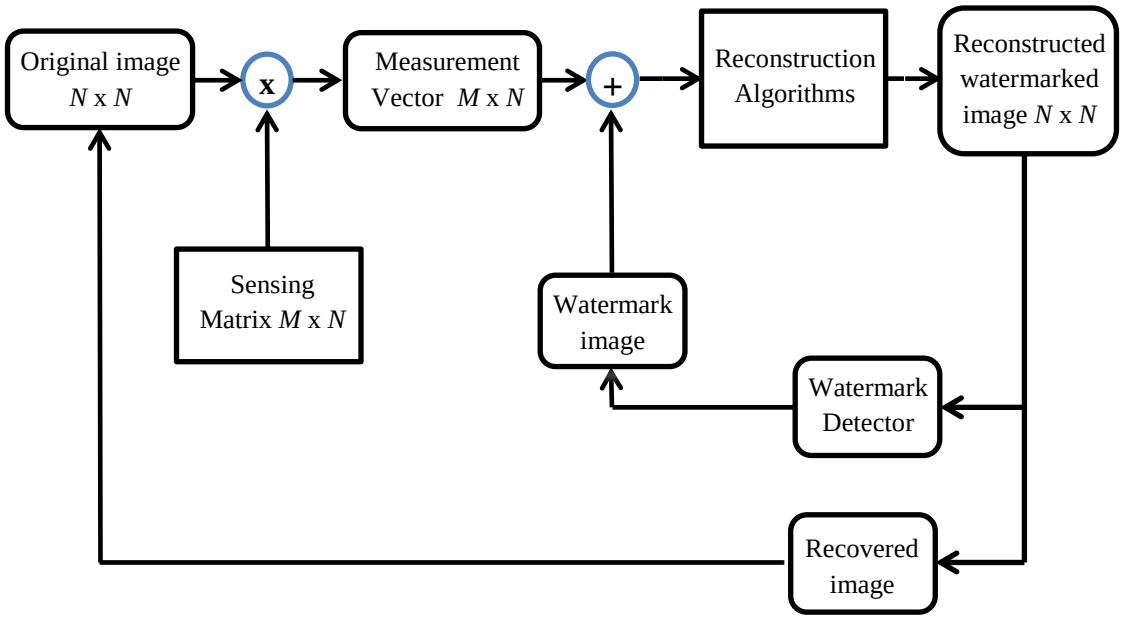

Figure 1.5. A scheme of CS watermarking procedure.

CHAPTER 2

OVERVIEW

2.1 Compressive Sensing CS

In this part, the overview of Compressive Sensing CS is displayed. Accordingly, some CS applications are explained.

2.1.1 Overview of Compressive Sensing CS

Compressive Sensing CS, also called Compressive Sampling, is an emerging area in information theory and signal processing that is attracting a lot of attention recently [11]. The motivation of using the compressive sensing is coming from the fact that the CS combines the sampling and the compression at the same time. In traditional recovery algorithms, to fully reconstruct a signal, it is sampled at a rate equal or greater than the Nyquist sampling rate. In different applications such as imaging, sensor networks, astronomy, high-speed analog-to-digital compression and biological systems, the signals are sparse in a certain basis.

The compressive sensing is used to reconstruct the high dimensional signals exactly by using much smaller measurements. Generally, the signals are represented by vectors in many applications like images or other objects. In the linear algebra theorem, many equations are unknown, thus the unique signal recovering from an incomplete set of linear vectors is not possible. As mentioned earlier, many signals are often sparse or compressible in some basis, these signals are represented as real world images or audio signals, and can accurately recover from incomplete linear measurements. However, the signal itself is sparse and non-trivial; thereby the compressed measurements are used to reconstruct this signal. The CS is utilized to recover the sparse signals from compressed measurements by efficiently and effectively decoding algorithms. One popular decoding algorithm is the Basis Pursuit algorithm [4].

The CS idea didn't come from anywhere, where the theoretical foundation of CS is dealing with high dimensional geometry and associated with the geometric functional analysis field. For example, Garnaev studied how many and what linear measurements are required to reconstruct vectors of CS by using the basic decoding method. By knowing the measurement matrix Φ, all solutions of x are in the underdetermined systems and are laid in an affine space parallel to the null space of Φ. Then Garnaev's problem clearly becomes a high dimensional geometrical problem, which is about how to select the null space so the affine space's intersection with the L1 ball has minimal radius [12]. Their pantheistic results depend on randomly choosing of the linear measurements and are optimized in order of a number of measurements, which is within a multiplicative factor of what the minimization compressive sensing supplies.

The deep probabilistic technique [13] is the generic chaining technique. This technique controls the upper of a random processes; these are used as an important technical tool in verifying that a certain measurement matrix ensembles satisfy the condition for recovering the sparse signals [14]. Compressive sensing has effects on the coding theory, such as in the error correlation problem over the real number field. The error correlation problem is considered a traditional problem in the coding theory. In the communications, the signals are sent from a sender to a receiver, these signals are corrupted by errors. Thus, these problems are taken into consideration when designing a system to correct the errors by using the decoding algorithms. The errors occur in a few places, so the sparse recovery reconstructs the signal by using the corrupted encoding data [7].

The error correlation problem happens in the real field, while the classical theory of coding supposes data in a finite field. In many practical applications, the encoding data happens in continuous real systems. The error correlation problem is formulated by exploiting the close relationship between the coding theory and CS. Let $v \in R^M$ is M dimensional input vector, the 'plaintext' that we hope to transmit depends on a remote receiver. N dimensional coded text is transmitted namely 'cipher text' where $z = \beta v$, β is $M \times N$ coding matrix. In case of no noise, if β has a full rank, the input vector v can recover from z. But in case of noise, z has been corrupted by sparse noises, the input

vector v recovers from the corrupted receiving code $z' = \beta v + e$, where $e \in R^M$ is the sparse error vector.

To understand that in CS setting, let Φ is a matrix that has a null space in range of β, then Φ applies to both sides of the equation $z' = \beta v + e$ to get $\Phi z' = \Phi e$. Set $y = \beta z'$, the problem is reconstructing the sparse vector e from the linear measurement y. The error vector e is reconstructed by the actual measurement Φx, if Φ is a full rank, the input signal v can recover. The starting point in the CS is an N dimensional signal vector that has a sparse representation in particular basis, assume $x \in R^N$ is N dimensional vector with K non-zero entries, $K \ll N$. Here, assume K can be up to a constant fraction of N, since this case is of great practical interest [7].

Compressive sensing has a recent study to receive a great amount of interested signals in the mathematics and signal processing application. The CS theory has been developed over the past few years. The recent researches show the major breakthrough explained under some sensible assumptions. By using the linear programming LP, the results could be practically feasible [15]. The method basically constrained L1-min has experimentally been known to implement well to find sparse solutions and shown in the literature as Basis Pursuit [4]. The compressive sensing area is closely connected to a related area of coding [7], high-dimensional geometry [16], the sparse approximation theory [17], data streaming algorithms [18] and random sampling [19]. Moreover, the compressive sensing applications are emerging in compressive imaging, medical imaging, sensor networks and analog-to-digital conversion [2].

CS is used in the sparse signal with a high dimensional space, CS connected both the sampling and the compression. Then the sparse signal exactly recovered from a fewer measurements that are a much less from it is a full dimension by sparse prior of the signal. Also, CS image is reconstructed by using the orthogonal matching pursuit OMP and the Matching Pursuit MP. The CS images must have a sparse representation in multi-wavelet transform domain. The Gaussian and Bernoulli matrices are used as measurement matrix [20]. The previous work compared between the CS and classical sampling. The CS directly sensed the data at a low sampling rate in a compressed form. The classical sampling theory focused on an infinite length and continuous time signal.

But the mathematical theory of CS focused on measuring a finite dimensional vectors in R^N and signal sampling at specific points in time [21].

2.1.2 Applications of CS

There are many applications for CS approach, we will review some of them as the following:

1-CS in Cameras

The block diagram of CS in Cameras is shown in Figure 2.1. Compressive sensing has a wide history in the compressive imaging systems and cameras. CS reduces the power consumption, computational complexity and storage space without losing the spatial resolution. With the single pixel camera appearance SPC by Rice University, the imaging systems altered significantly. The camera is based on a single photon detector adaptable with the image at wavelengths, which were impossible with conventional CCD and CMOS images [22]. The CS used to reconstruct an N x N sparse image by fewer than N^2 measurements. In single pixel camera SPC, each mirror in Digital Micro mirror Device DMD array implements two of the following tasks: either reflect light towards the sensor or reflect light away from it. Thus the light delivered at the sensor (photo diode) end is a weighted average of many pixels; this combination provides a single pixel.

When N measurements are taken with random selection of pixels, SPC acquires a recognizable picture similar to N pixel picture. The single pixel camera SPC is used in the color images (hyper spectral camera) in combination with Bayer color filter [23]. The SPC captures the data, when it is used for background subtraction for automatic detection and tracking of objects. In a sequence of video frames, the foreground objects separate from the background. But it is more expensive in the wavelengths than the visible light. Compressive sensing solves the problem of vision applications. The natural images are sparsely represented in wavelet domains [24]. In CS, the random projections of a scene are taken to an incoherent set of a tested function and reconstructed by solving the convex optimization problem or Orthogonal Matching Pursuit algorithm. CS measurements also decrease the packet drop over the communication channel. In the

recent works, the design of Tera hertz imaging systems is proposed. In these systems, image acquisition time is relatively connected with the speed of the THz detector. The proposed systems remove the need for Tera hertz beam and have a faster scanning of object [25].

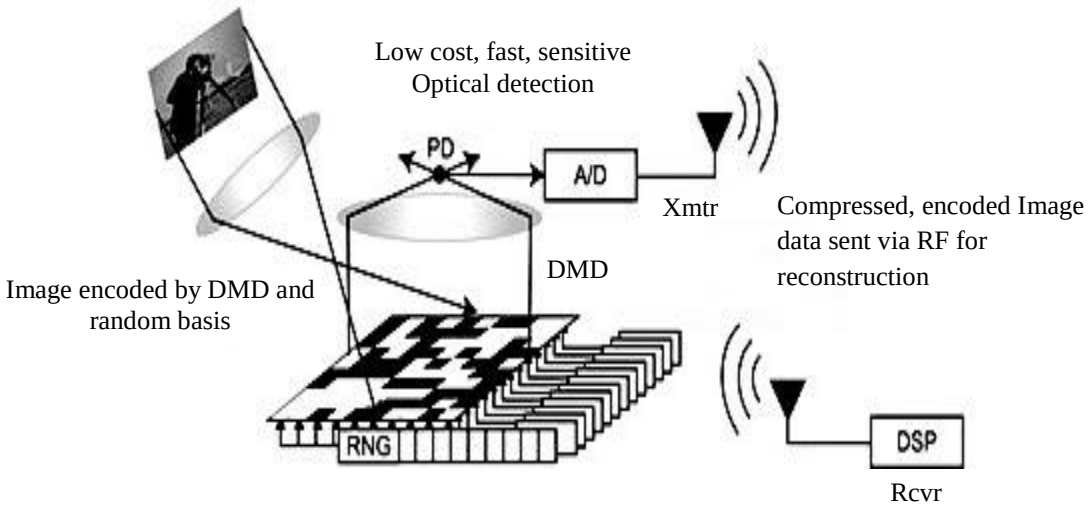

Figure 2.1. Block diagram of Compressive Imaging Camera [22].

2- Medical Imaging

In the medical imaging, the compressive sensing has an active pursue in the different applications such as the Magnetic Resonance Imaging MRI. MRI images are used in the different applications like angiograms. The MR images have Sparsity properties in Fourier domain or wavelet basis domain. The MRI is time consuming because of the data collection processes, which depend on physical and physiological constraints, but the CS technique improves the image quality by reducing the number of the collected measurements and uses their implicit Sparsity later. The MRI has wide research area in the CS community, and there are some CS algorithms, particularly designed for this purpose [26].

3-Seismic Imaging

The seismic images are not sparse or compressible images. However, by using the transform domains e.g. the curvelet basis, the seismic images can be altered to compressible images [27]. Seismic data has a high dimensional and incomplete properties. In the seismology detection techniques, the collection of massive data volume requires, which is represented at five directions: one for a time, two for sources and two for receivers. These numbers of sources and receivers must be reduced, because they have high measurements and computational cost. At the same time, the number of samples is also reduced. The sampling technique needs a fewer number of samples. At the same time, the image quality must be saved. CS treats with this problem by implementing the sampling and the encoding techniques at one step by reducing their dimensions. This randomized sub sampling is useful because the linear encoding does not require high resolution information. The reconstruction theory of CS has been developed like Curvelet Based Recovery by using the Sparsity Promoting Inversion CRSI [28].

4-Biological Applications

The CS approach is used in biological applications, because it has efficient and inexpensive sensing. The idea of group testing is closely related with CS. It was used for the first time in World War II to test soldiers for syphilis [29]. Because testing for syphilis antigen in the blood is costly, instead of testing the blood of each soldier alone, the used method was grouped of the blood samples had been taken from the soldiers and these samples were tested together. The recent works used the CS in comparative DNA microarray [30]. Classical microarray bio-sensors are only beneficial for discovering the limited number of microorganisms. The DNA microarrays are described by millions of probe spots to check a large number of goals in a single experiment. In classical microarrays, the single spot is described by a large number of copies of the probes designed to capture single goal and hence its combined data of a single data spot. CS provides alternative design for the compressed microarrays [30], whose each spot has copies of various probe sets to reduce the total number of measurements and still efficiently recovery implemented for them.

5-Compressive Radar

The CS theory is used in the Radar system design by removing the need for of pulse compression matched filters at the receiver, and decreasing the analog to digital conversion bandwidth from Nyquist rate to information rate. CS is used to simplify the hardware design [31]. Also, CS provides a better resolution through traditional Radars, the resolution can be restricted by time-frequency uncertainty approaches [32].

The resolution of any signal is improved by using the following serial approach: transmitting an incoherent deterministic signals, eliminating the matched filter and recovering a received signal using Sparsity constraints. CS is used to increase the resolution of a wide angle synthetic aperture Radar [33]. The CS techniques are used in the following applications: mono-static, bi-static and multi-static Radar. The CS image is used in the sonar and ground Penetrating Radars GPRs application [34]. Also, the CS enters in the detection of human motion identification through the wall imaging.

6-Analog-to-Information Converters

In the communication systems, high bandwidth RF signals are used at a rate enough to sampling these signals. The information contained in the signals is much smaller than the bandwidth of these signals in different applications. This problem is solved by the CS approach, which converts the Analog signal to Digital by Analog to Information Conversion AIC approach. In the Analog to Digital converter ADC, the random non uniform sampling approach is used in the bandwidth limited to present the hardware devices [35]. AIC approach uses random samples in wideband signals for which random non uniform sampling fails.

The AIC establishes three basic components: demodulation, filtering and uniform sampling [36]. The random demodulator is described by using the limitation to discrete multi-tone signals and incurred high computational load [37]. In the AIC, the random filtering is used and it needs less storage and computation for measurement and recovery [38]. The modulated wideband converter is described in the recent works; it has three basic components: low pass filtering, uniform sampling at low rate and multiplication of analog signal with bank of periodic waveforms [39].

2.2 Overview of Reconstruction Algorithms

2.2.1 L1 minimization algorithm

L1 minimization is an optimization method used in the signal or image reconstruction by the underdetermined systems in a long history. L1 minimization is heard of many statistical and numerical analysis algorithms. These algorithms are utilized for compression, approximation and statistical estimation. Sometimes, L1 minimization norm is used as Sparsity promoting function that is found in the convolution of seismic traces and reflection seismology. The L1 minimization has accurate results and begun to emerge in the early stages [40]. The statistical application of L1-minimization algorithm began in the mid-1990's with the introduction of the least square absolute shrinkage and selection operator LASSO and related formulations [41]. The iterative soft-threshold, also known as Basis Pursuit [42] is used in the compression applications to decode the sparsest signal from high complete frames.

In addition, L1 minimization algorithm is used by the signal processing groups for the sparse signal analysis [43]. The basic theory of CS consists of two components: recoverability and stability. The recoverability has a basic question: what types of the measurement matrices and reconstruction procedures include an exact recovery of all *K*-sparse signals (where have *K*-nonzero), and how many measurements are sufficient to guarantee such a recovery? The stability and robustness exist in the reconstruction methods when the measurements are noisy and / or Sparsity. The new researches explained that the certain matrices can guarantee reconstruction by using the L1 minimization when the Sparsity *K* up to order of $\sqrt{M}$ [7].

These researches show that the standard normal random matrix $\Phi \in R^{MxN}$ is recovered by a high probability for Sparsity *K* up to order of *M*, where *M* = (*K*) log (*K/N*), which is the best recoverability order available [14]. In practice, almost all cases take the measurements as noisy or take the signal Sparsity as inexact or both. The signal is represented as the inexact Sparsity case if this signal has a small number of coefficients in the magnitude. The subject of CS stability studies the CS approach accuracy in the signal reconstruction. This stability is taken by L1 minimization algorithm:

$$\min \{ \|x\|_1 : \|Ax - b\|_2 \leq \gamma \}. \qquad (2.1)$$

where $b = A\hat{x}$, $\hat{x}$ is approximately K sparse and only has K significant components, assume $\hat{x}(K)$ is a best K term approximation of $\hat{x}$ and obtaining by setting $N - K$, where N is insignificant components of $\hat{x}$ setting to zero. Let x^* be the optimal solution for L1 minimization algorithm. The stability results of L1 minimization can be seen in following two types of error bounds:

$$\|x^* - \hat{x}\|_2 \leq CK^{-1/2} \|\hat{x} - \hat{x}(K)\|_1. \qquad (2.2)$$

$$\|x^* - \hat{x}\|_2 \leq C \|\hat{x} - \hat{x}(K)\|_1. \qquad (2.3)$$

The Sparsity level K is order of M, where M= log (K / N) and it depends on the type of measurement matrices which are in use, C is a constant and can vary from one case to another, then C is established by some works [14, 44]. The stability result case in L1 minimization method (2.1) extends in the work [44] as:

$$\|x^* - \hat{x}\|_2 \leq C(\gamma + K^{-1/2} \|\hat{x} - \hat{x}(K)\|_1), \qquad (2.4)$$

where $\hat{x}$ represents the exactly K-sparse and $\hat{x} = \hat{x}(K)$, the stability results in the previous equations (2.3), (2.4) reduce the exact recoverability, whose $x^* = \hat{x}$, also $\gamma = 0$ required in the equation (2.4). The stability results in the equation (2.4) imply recoverability if it is combined with pertinent random matrix properties. The more recent work explains the stability results establishment by using L1 minimization algorithm and some greedy algorithms [45]. Today, the CS approach has recoverability with unknown stability. The CS recoverability and stability results are primarily based on analyzing properties for measurement matrix Φ, and Φ matrix must satisfy the Restricted Isometry Property RIP. RIP is an analytic tool which is most widely used in measurement matrix Φ satisfying. The RIP is firstly introduced for the CS recoverability analysis [7], but an earlier usage is found in [46]. Donoho explains the stable reconstruction of L1 minimization under three conditions: namely conditions CS1-CS3 on measurement matrix Φ. These conditions do not use RIP properties directly; CS1 condition is used in the minimum

singular values of a sub-matrices that are represented as M x K, with $K < \rho M / \log(N)$ for some $\rho > 0$, $\Phi \in R^{MxN}$ is uniformly bounded under from zero. Thus, the stability results depend on a matrix Φ [4].

Another work studies another analysis tool; it includes the combinatorial and geometric properties of the polytypic fashion by using Φ columns. But RIP approach uses sufficient conditions for the recoverability [47]. The stability results in (2.2) and (2.4) are coming from the polytypic approach, which used a necessary and sufficient condition. The last approach leads to tighter recoverability constants. The minimum L1-norm criterion is used to produce accurate results and many researchers indicate that. The minimum L1-norm is used to recover a sparse spike from its partial spectrum information and this result is mathematically proven. Also the L1-norm minimization method is used to reconstruct the sparse signals in ultrasonic nondestructive evaluation application area [43].

David Donoho explains the theoretical explanation to why the minimization L1- norm is used to reconstruct sparse signal [46]. Also, another work makes great contributions in the same area [48]. Other researchers are putting their results in the accurate image recovery from highly incomplete frequency information. They suggest the Uniform Uncertainty Principle UUP concepts together with the restricted isometry constant δ to support their work [15]. Team of Digital Signal Processing DSP at Rice University mentioned the signal pixel camera recovery, and they understood the sparse signal reconstruction by the CS theory experimentally.

2.2.2 Orthogonal matching pursuit OMP

In the communication and signal processing systems, the data compression approach is considered a crucial process because of the limitation on the amount of the data. One of compression methods expands the information over a complete signal space, which searches about the sparse representation with a small number of nonzero. Also the compression method tries to find a sparse solution of linear systems, which is a nondeterministic polynomial time NP hard problem [49]. The greedy algorithms are considered as a simpler solution; it needs a sequential selection of basis vectors form set

a of the over complete vectors called a dictionary. These algorithms are known as Sequential Basis Selection SBS algorithms. One type of SBS algorithms is the Matching pursuit MP. It is used in a signal and image reconstruction [50]. There are some usages of MP algorithm in the practice shown in the video coding [51].

Orthogonal Matching Pursuit OMP is a greedy algorithm developed from the MP. It is widely used for sparse signals recovery from compressed measurements. It is an alternative method used to find the target vector x from the measurement vector y as shown in Table 2.1. OMP algorithm takes many steps from MP and makes some essentially modification for these steps. These modifications are represented by using a least square formulation to obtain the best approximation for the measurement vector y over the selected columns. The column indices kept by the OMP algorithm at a set known as the active set I. Thus, the selected columns are called active columns as explained in Table 2.1. The OMP approach just like MP begins from all zero solution, then initializes the residual to measurement vector y. In each iteration, columns of sensing matrix Φ are selected. These Φ columns must have a good correlation with the residual vector r. Then index of the selected column is added into the active set I.

The active entries are the active set I. In the next step, the active entries of the solution vector x are found by solving the least square problem over the active columns. The final solution of OMP algorithm is represented by the orthogonalization step. In this step, the OMP algorithm is faster and columns of measurement matrix Φ are selected one time more than the traditional MP algorithm. Therefore, the MP approach requires a number of iterations more than the OMP approach to reach the final solution. In each iteration, the OMP algorithm has a higher computational cost than the MP algorithm iteration. The reason for that is the orthogonalization step, which provides the least square problem solution in the OMP algorithm.

Table 2.1. Orthogonal Matching Pursuit OMP algorithm**.**

Inputs	
Initialization:	measurements y
	Sensing matrix Φ

	Sparsity K. Iteration count $k = 0$ Residual vector $r_0 = y$ Estimated support set $I_0 = \Phi$.
Procedure	
While $k < K$	
	$k = k + 1$. $a_k = argmax_i \lvert\langle r_{k-1}, \varphi_i \rangle\rvert$. $I_k = I_{k-1} \cup \{a_k\}$. $\hat{x}_{I_k} = arg\ min_{\ x}\ \left\lVert y - \phi_{I_k} x \right\rVert_2$. $r_k = y - \Phi_{I_k} \hat{x}_{I_k}$.
End	
Output	
$\hat{x} = \underset{x:supp(x)=I_k}{\arg\min} \left\lVert y - \phi x \right\rVert_2$	

OMP algorithm has a high probability to reconstruct K sparse signal which contains K nonzero entries, and the vector y with the matrix Φ are used at most K iterations [5]. The OMP approach finds an efficiently sparse solution of the underdetermined linear systems by using a small Sparsity K. The Sparsity K of any vector is indicated by nonzero entries number in the same vector. The Forward Stepwise Regression FSR algorithm is the same as the OMP algorithm in the statistical literature [52]. The OMP algorithm is used to solve a linear equation, which reconstructs the sparse signal. The algorithm is genius to solve the percent damage in few numbers of element cases. The OMP approach chooses the damaged entries one by one. This method is used to cope with the noise and error case through the reduction model. Another researcher uses the Complementary Matching Pursuit (CMP) algorithm for a sparse approximation. The CMP method is the same as MP method, but it takes the row space of a sensing matrix in the implementation. The CMP has a similar sub-optimality problem just like the MP method

[53]. The Orthogonal Complementary Matching Pursuit (OCMP) algorithm is used to solve this problem which tries to eliminate the sub-optimality by updating elements of the selected atoms at each iteration.

The OCMP approach is a developed case of CMP approach, where it uses the same OMP procedure, but the residual errors that result from using OCMP are not orthogonal to the selected atoms up to competent iteration. In the OMP approach, the residual energy increases through the first iteration, while in the OCMP approach, the convergence speed increases in the next iteration and it improves the Sparsity of the solution vector. The OMP algorithm has a low cost in different applications. Therefore, it is used instead of the linear programing LP algorithm. The Generalized Orthogonal Matching Pursuit (GOMP) is derived from the OMP [54]; this is proposed to generalize the OMP through various N indices identified per iteration. The GOMP approach is finished with a few numbers of iteration than the OMP, and exactly recovers K sparse signals.

A number of studies about the insertion of some modifications to OMP approach are available; these modifications improve the computational efficiency and recovery performance of OMP. These studies propose a method, where in each iteration more than one indices are identified. This method is called Stage-Wise Orthogonal Matching Pursuit STOMP, which selects a correlation magnitude surpass the deliberately designed threshold. The benefit of that is shown when comparing it with L1-min technique, where it is faster than the L1-min [55].

There is another method which is different from the OMP approach and known as Regularized Orthogonal Matching Pursuit (ROMP) [45]. This method shrinks the candidate through choosing a subset which satisfies the predefined regularization rule. Also, the ROMP approach provides an accurate reconstruction of K sparse signal. In general, the MP method is more powerful than the OMP method. But the OMP method has a better computationally efficient and an easy implementation. The OMP method has an additional benefit where it seeks the sparsest solution, and it stops after number of selected Φ columns. Thereby the OMP is used for the sparse signal reconstruction.

The OMP is proposed as simplicity and fastness for a high-dimensional sparse signal reconstruction, which has simply realized the reconstruction process in the practice [56]. The performance of OMP approach has proved its ability to reconstruct the sparse signals with high probability; where the OMP starts by finding column of measurement matrix Φ, then this step is repeated by correlating columns of the measurement matrix Φ with the signal residual r, which is implemented by subtracting the partial estimation of the signal from the original measurement vector [5].

The classical signal representation methods use the orthogonal bases to represent the signals. These methods decompose the arbitrary signal into a linear expansion of the waveforms, which choose a bigger and a redundant family of functions known as dictionaries. These dictionaries are recovered by using a frame structure [57]. The MP and OMP approaches are used to reconstruct these dictionaries [4]. The MP algorithm is used to represent the sparse signal by selecting a dictionary atom, which is adapted with the approximation part of a signal at each iteration. The MP approach does not have a linear expansion of the selected atoms; it is used in the signal approximation, while the OMP algorithm is used to increase a set of coefficients. These coefficients result from a linear expansion that reduces the distance of a signal to minimize residual of the new approximation [58].

Some researchers suggest another approach to show the performance of OMP in the exact support reconstruction through certain restricted isometry property RIP assumptions [4]. Authors proposed [59] the optimized orthogonal matching pursuit with the OMP approach. These algorithms are introduced by using the optimization and the orthogonal projections. The optimization approach selects the atoms with a minimum number of approximation error, while the orthogonal projection takes the OMP properties. That the data vector and the dictionary atoms are projected onto orthogonal subspace spanned of the active atoms. Also the orthogonal projection selects the normalized projection atoms which have the largest inner product with the residual data. In each iteration, the amount of the active atoms is increased by one.

2.2.3 Orthogonal Matching Pursuit with Partially Known Support OMP-PKS

By prior information, the noise tolerance may be increased. The wavelet tree structure has a public knowledge in the model of a sparse signal [60]. This model is used in the recovering methods that have three benefits: reduction in the number of measurements, increase in robustness and the faster iterative signal recovery from incomplete and inaccurate samples. OMP-PKS is a greedy algorithm which is used in the sparse signal or image reconstruction [6, 61, 62]. The OMP-PKS algorithm is developed from the traditional OMP algorithm [5]. The OMP-PKS approach has a partially known support property exploited in the sparse signal or image reconstruction.

The partially known support PKS part provides a priori information to determine whether any sub-band in the sparse signal is more important than the other sub-bands. The important sub-bands are selected as non-zero elements. The OMP-PKS algorithm, similar to the OMP satisfies the Restricted Isometry Property (RIP) and the requirement of RIP is not as sharp as BP [1]. The OMP-PKS approach has fast implementation and it requires very low measurement rates. OMP-PKS algorithm is different from the Tree-based Orthogonal Matching Pursuit (TOMP) algorithm [8], which does not use the previously selected bases in the next basis selection. But the TOMP selects a best next wavelet sub-tree and set of atoms in the wavelet tree.

In the last years, the recent works have used the basic concepts of the CS and modified them to include the partially known support PKS idea in sparse or compressible signal reconstructions. One of these works modified three greedy methods to combine the partially known support idea with the reconstruction approaches. The activity and performance of using the prior data are studied. Then the result has showed a high performance of the modified greedy methods, which need a few number of samples for the approximated reconstruction [6]. In other works the priori information idea is exploited to minimize the number of samples in a sparse image or signal recovery, which uses the known subspace model or known graphical model ideas for the signals then mixes these models with the recovering methods to implement an exact few samples reconstruction [63]. In the OMP-PKS algorithm, the portion of a signal is priori

known and tries to evaluate the unknown support part which is a sparser signal than the original [62].

As in the recent works, the CS framework has been modified to give prior knowledge supports, which are used to improve result of reconstruction a fewer measurements [61]. The modified compressive sensing demonstrates the measurements whose support include a smallest number of new samples T_0 as shown in the equation (2.5), which modified the Basis Pursuit (BP) algorithm [62] to explain the sparse signal by supposing the uncorrupted measurements. This method has been expanded to prove the stability results from using the corrupted measurements and compressible signals [61]. OMP-PKS algorithm solves the following optimization program:

$$\min_{x \in R^n} \left\| x_{T_0^c} \right\|_1 \quad \text{Subject to } \left\| y - \phi x \right\|_2 \leq \epsilon. \qquad (2.5)$$

A recent work proposed a robust reconstruction approach that used the compressed signal ensemble from one compressed signal. The compressed signal is represented as sub samples for *t* times to generate the ensemble of *t* compressed signals [64]. The OMP-PKS is implemented to each ensemble signals to recover *t* noisy outputs, whose *t* is a noisy output averaged for denoising. A new CS recovery approach has been designed. This approach used the known support ideas to recover the sparse image. The performance of this new method compared with the basis pursuit denoising methods [64].

The sparse recovery problem with the noiseless measurements is studied [62]; the portion of the signal support is known. This known part may have some errors. The prior knowledge provides the known support portion. In the Magnetic Resonance (MR) image, the Discrete Wavelet Transform (DWT) is used to convert this image into a sparse image. After that, the image has the fewest black background known as detail part and other most coefficients are nonzero. These coefficients are obtained as approximation coefficients, and then the indices of these coefficients are called known support part [65].

All nonzero elements of the sparse signal in the Sparsity basis can be altered through time. Then the new coefficients will be nonzero. So the Sparsity size becomes equal or larger than the original signal. Therefore, the reconstruction of this signal by few measurements becomes not exact [66]. Table 2.2 explains the OMP-PKS algorithm, which shows and explains the Partially Known Support (PKS) part, where Φ is the measurement matrix, y is the measurement vector, z is the PKS part with indices $\{\gamma_1, \gamma_2, \gamma_3, \ldots\ldots, \gamma_{|z|}\}$.

Table 2.2. Orthogonal Matching Pursuit with Partially Known Support (OMP-PKS) algorithm.

Input
$\Phi = [\varphi_1\ \varphi_2\ \varphi_3 \ldots\ldots\ldots \varphi_N]$. y: measurement vector. The Sparsity level K. $z = \{\gamma_1, \gamma_2, \gamma_3, \ldots\ldots, \gamma_{\lvert z\rvert}\}$.
Procedure
Selection without correlation test. 1- Select every basis of the known part. $t = \lvert z\rvert$. $\eta_t = z$. $\Phi_t = [\varphi_1\ \varphi_2\ \varphi_3 \ldots\ldots\ldots \varphi_t]$. 2- Solve the least square problem to obtain the new reconstructed signal, z_t. $z_t = argmin_z \ \lVert y - \phi_t z \rVert_2$ 3- Calculate the new approximation a_t, and find the residual r_t, which is the projection of y on the space spanned by Φ_t. $a_t = \Phi_t z_t$ $r_t = y - a_t$

Output
The reconstructed signal $\hat{x}$ The set containing K indexes of non-zero element in $\hat{x}$, $\eta_k = \{\lambda_1, \lambda_2, \ldots\ldots, \lambda_K\}$

2.3 Watermarking image

2.3.1 Overview of Watermarking Image

Digital watermarking has embedding data process in a certain digital signal. The digital image is known as a cover or host image. The digital watermarking innovation traces back to 1954. Some of works in the watermarking technique got a patent by describing an approach for music signal identification through inaudible codes embedding [67]. The digital watermarking interest began in the early/mid-nineties, and then started to grow significantly. Digital watermarking techniques were used fundamentally in the intellectual property rights protection in the digital work [68]. Different embedding algorithms were developed for inserting variety information into still images, videos, texts, audio and digital circuits [69, 70].

Digital watermarking became a very important research field with a promising future, as evident in a number of workshops, in different conferences and journals about the watermarking research. The digital watermarking is considered as an open topic, and far from being a mature technology. Digital watermarking technologies could not handle some problems in the Digital Rights Management field. The digital watermarking is exploited by some companies in different applications such as broadcast monitoring, audience metering, or audio and video watermarking. Some companies merged the watermarking capabilities to their video surveillance solutions like GeoVision [71], MediaSec [72] and TRedess [72]. The recent researches exploited the digital watermarking and fingerprinting techniques in many experiments [73]. Few works make reference to combine the watermarking and compressive sensing systems. One of these works is an innovated method to protect copyright information with the compressive

sensing. In that work, the relationship between the coefficients is carefully taken. A few numbers of transmitting coefficients are able to recover the image. The secret data are inserted into the image before reconstructing it by using the reconstruction approaches [74]. Another watermark insertion technique explained that the watermarked image is detected in some degree at the receiver with keeping the robustness. This method is used to protect a copyright of the original multimedia contents. In addition, the watermarked image quality must be reasonable with the compressive sensing [75].

The digital watermarking method with the CS approach takes three process steps: compression of the compressive sensing process, compressive sensing reconstruction process and compressive sensing extraction. The watermarking image is embedded by utilizing the embedded procedure between compression of the compressive sensing process and the compressive sensing reconstruction process. The proposed method has robustness in the performance [76]. Another work proposes the watermarking image procedure in the compressive sensing, which is used the random selection measurements from image blocks to insert the watermark [77].

The image reconstruction approach requires a set of watermarked measurements that are implemented by the total variation minimization TV min method. The reconstructed image has a high quality, and the extracted watermarking image from the reconstructed image has a high accuracy. Another researcher analyzed the performance of the watermark extraction method through the CS. The watermark image is generated by using the pseudo random sequence. Then it is inserted into coefficients of the Discrete Cosine Transform (DCT) image. The watermarked image is reconstructed by using a good quality CS reconstruction method with a small number of samples. These samples are generated from the low frequency DCT coefficients [78].

2.3.2 Watermarking properties

The watermarking systems have many important properties. Some of these properties are often conflicted and often forced to accept some trade-offs between these properties; they depend on the watermarking system applications. The first property is the effectiveness and it is a very important property. This property ensures the successful

detection of a message from the watermarked image. The second property is the image fidelity. The watermarking approach is used to add a message into a host image, so it inevitably affects the image quality. Therefore, the degradation of the image quality must be kept to a minimum value, so no obvious difference is observed in the image fidelity. The third property is the payload size. In the watermark embedding algorithm, the watermarked image carries a message; this message size is very important in many systems, which require a relatively large payload to be embedded in a covered work. Other applications need a single bit to be embedded. In the watermarking systems, the false positive rate is also very important. There are a number of digital works which have a watermark embedding, but in the fact there is no watermark embedding. Therefore, this case should be kept low in the watermarking systems. Lastly, robustness has been widely used in the most watermarking systems. The watermarked works are altered during their lifetime in many situations: either by the transmission case over a lossy channel or by several malicious attacks, which try to eliminate the watermark or make it undetectable. The robust watermark must be capable of resisting the additive Gaussian noise, compression, printing and scanning, rotation, scaling, cropping and many other operations.

2.3.3 Application of the digital watermarking

In this section, some digital watermarking applications are explained as follows:

1-Signatures

The owner of the content is identified by the watermark. This information helps the user obtain legal rights to copy or publish a data from the contact owner. It may be also used to settle the ownership disputes.

2-Fingerprinting

The watermark is utilized to identify the content buyers. This may help in tracing the source of illegal copies, which are executed in the Digital Video Disk Players (DVDP), whose watermark is put in each of it, then it identifies the player in each movie that is played.

3-Broadcast and publication monitoring

As in the previous case, the watermark identifies the owner of content, while here automated system is applied to detect the watermark as in the computer networks, monitor, television, radio broadcasts and any other distribution channels to save track of when and where the content is shown. The Music-Code system prepares broadcast monitoring of an audio, VEIL-II and MediaTrax are preparing broadcast monitoring of a video. European project known VIVA began to develop the watermark technology for a broadcast monitoring.

4-Authentication

The watermark encodes information needed to show that the content is authentic. It is designed in a way that any content change either destroys the watermark, or does a mismatch between the content and the watermark, which is easily uncovered. If the watermark matches the content, the user of the content can be sure that it has not been altered since the watermark is inserted.

5-Copy control

The watermark provides information about the usage rules and copying where the content owner hopes to enforce. These are simple rules like “this content may not be copied”, or “this content may be copied, but no next copies may be made from that copy. The devices which are able to copy that content require a law or a patent license to check for, and abide by these watermarks. Also, the devices that can play the content may be checked for the watermarks and compared with other clues, e.g., whether the content is on a recordable storage device to identify illegal copies and refuse to play them. This is the application that is currently envisaged for Digital Video Disks (DVD).

6-Secret communication

The secret information is transmitted from a person or computer to another by using the embedding algorithm, and along the way no one will know that this information is being sent. This represents the traditional application of steganography. Simmons works are motivated by the Strategic Arms Reduction Treaty verification. Electronic detectors

provide transmitting the status (loaded or unloaded) of a nuclear missile silo, but not the position of that silo. It applies the digital signature schemes that are intended to explain the integrity of such a status message, misused as a”subliminal channel” to pass a long espionage information [79].

Many general domains and shareware programs are available to provide the watermarking for the secret communication. Some related works suggest that the availability of the technology casts serious suspicion on the effectiveness of government limitation on encryption, since these limitations cannot be implemented to steganography [57]. The watermark has some major applications which are currently being explained or used. However, many others which appeared in a full implication of this technology are realized.

CHAPTER 3

METHODOLOGY

In this work the watermarking algorithm is utilized to protect the watermarking image in the compressive sensing CS. The watermarking algorithm uses the encoder and decoder procedures to insert and extract the watermarking image. The watermarking image inserts into the measurement vectors that result from applying the CS approach for the sparse image. The resulting watermarked measurement vectors are reconstructed by using three reconstruction algorithms: L1 minimization (L1-min), Orthogonal Matching Pursuit (OMP) and Orthogonal Matching Pursuit with Partially Known Support (OMP-PKS). After reconstructing the watermarked measurement vectors, a best decoder procedure is applied to extract the watermarking image again.

In this chapter, firstly CS has been considered and accordingly a basic explanation of CS has been given. Then the proposed reconstruction approaches have been discussed. Finally, efficient watermarking encoder and decoder methods, and the proposed flowchart considering all the used algorithms with the procedures have been discussed, respectively.

3.1 Compressive Sensing CS

CS [1, 2] handles the signals or the images that are sparse in a certain transform domain. It means that the signals have a brief representation in a suitable basis. In general, a signal which has *K* sparse can be exhibited by M measurements, where $K << M << N$, *N* is the number of columns in the measurement matrix Φ, expressed as samples in the Shannon-Nyquist theorem. If x is a discrete signal with length *N*, then the signal *x* can be shown in basis vectors as:

$$x = \sum_{i=1}^{N} \psi_i f_i = \psi f \tag{3.1}$$

where f_i is the transform domain components, Ψ_i represents as a basis vector by N x N transform matrix, Ψ_i columns are orthonormal basis. Although, the dimension of the signal reduces, the needed data must be enough for reconstructing the signal to be similar to the original signal. The sensing matrix $\emptyset \in R^{MXN}$ has an incoherence characteristic together with the basis matrix Ψ. The coherence defines as a measurement of the largest correlation between two columns in the measurement matrix $\emptyset$ or between two matrices as shown below:

$$\mu(\emptyset, \Psi) = \sqrt{N} \max_{k \geq 1, j \leq N} \left| \left\langle \varnothing_k, \psi_j \right\rangle \right|. \quad (3.2)$$

where N represents the length of the signal, $\emptyset_k$ and Ψ_j are taken as column and row vectors of $\emptyset$ and Ψ matrices respectively. The coherence can be appeared in the range:

$$1 \leq \mu(\emptyset, \Psi) \leq N. \quad (3.3)$$

When the columns and the rows are correlated with a high value, which leads to reduce the coherence, then the low coherence between $\emptyset$ and Ψ mean that the number of measurements is needed to reconstruct the signal will be reduced. These numbers are estimated by using the following equation:

$$M \geq O(K) \log(N / K). \quad (3.4)$$

where O is a constant. When the number of measurements is small compared with the signal length as shown in Figure 3.1, the measurement matrix is called underdetermined matrix because the number of rows are less than the number of columns in the measurement matrix. This means the number of equations are less than the number of unknown variables. Therefore, there are some dependent variables together with the free variables in the underdetermined matrix systems. The measurement matrix is used to compute the measurement vector y as shown below:

$$y_{Mx1} = \emptyset_{MxN}\, x_{Nx1}. \quad (3.5)$$

From (3.1) and (3.5) produce the linear equation system which contains M equation together with N unknowns, $M << N$, as follows:

$$y = \emptyset\, x = \emptyset\, \Psi f = \Phi f. \tag{3.6}$$

To get the optimal solution, the underdetermined system has been used with many (infinite) solutions. The equation (3.5) is underdetermined when $K < M \ll N$, if the matrix Φ satisfies the Restricted Isometry Property (RIP), $\hat{x}$ can be reconstructed exactly by a suitable reconstruction algorithm. Candès and Tao [7] introduce RIP as follows:

Definition: A matrix Φ satisfies RIP of order K if there exists a $\delta_k \in (0, 1)$ such that:

$$(1-\delta_K)\|x\|_2^2 \le \|\phi x\|_2^2 \le (1+\delta_K)\|x\|_2^2. \tag{3.7}$$

If Φ satisfies the RIP of order $2K$ with $\delta_{2K} < \sqrt{2} - 1$, the K sparse vector x given in equation (3.6) can be reconstructed as explained in the Figure 3.1 by using the reconstruction approaches.

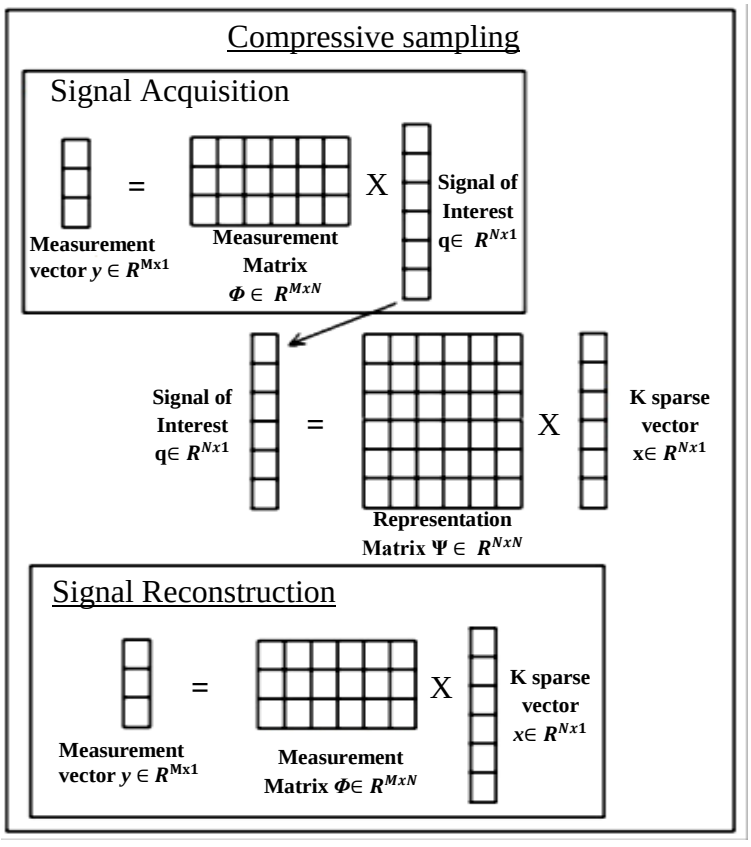

Figure 3.1. Compressive acquisition and reconstruction [80].

3.2 The reconstruction algorithms

Three reconstruction algorithms L1-min, OMP and OMP-PKS, are used to reconstruct the sparse image.

3.2.1 L1 minimization algorithm

The L1 norm minimization is an optimization linear programing (LP) algorithm, that solves the underdetermined systems shown in equation (3.6), where $\hat{x}$ is estimated by applying pseudo-inverse of the measurement matrix Φ into the measurement vector y as explained below:

$$\hat{x} = \min_x \|x\|_{l_1} \text{ . Subject to } \Phi x = y \text{ and } \Phi x - y = 0. \qquad (3.8)$$

Then $\hat{x}$ is exactly recovered. The L1 minimization gives the same results as L0 minimization in a different case of practical interest. L1 minimization method also approximately recovers the compressible signals. The L1 minimization is also known as a convex optimization program. This convex optimization program is often called Basis Pursuit BP [4]. In compressive sensing, the measurement number M is smaller than the signal length N, $M \ll N$. In this situation, the equation (3.5) is ill posed not immediately solved. If the signal x has K sparse (where the relationship between K and M defined in equation (3.4)) which means the cardinality of the signal is smaller or equal to K, the sparse signal x can be reconstructed from K measurements by solving L1 minimization problem as shown in equation (3.8)

3.2.2 Orthogonal Matching Pursuit (OMP)

The OMP is a greedy algorithm developed from the matching pursuit MP [51, 58]. It is used in the image reconstruction by estimating $\hat{x}$ over number of iterations. The OMP approach similar to MP begins from all zero solution, then initializes the residual r into the measurement vector y. In each iteration, columns of sensing matrix Φ are selected. These Φ columns must have a best correlation with the residual vectors r. Then index of the selected columns is added into the active set. The active entries correspond as the active set λ as shown in Tables 3.1 and 3.2 (part two). In the next step, the active entries

of the solution vector *x* are found by solving the least square problem over the active columns:

$$r = y - \Phi x \leq \epsilon. \tag{3.9}$$

$$x_t(\lambda) = argmin_v \left\| y - \Phi_\lambda x \right\|_2^2. \tag{3.10}$$

where ϵ is a minimum error value, Φ_λ is a sub-matrix formed by the active columns, $x_t(\lambda)$ is a sub-vector formed by the active entries of the vector *x*. The equation (3.10) is solved by finding the projection of vector *y* onto the space spanned by the active columns, and that needs a good knowledge of the linear algebra techniques. Also $x_t(\lambda)$ solving is achieved by the following equation:

$$\Phi_\lambda^T \Phi_\lambda x_t(\lambda) = \Phi_\lambda^T y. \tag{3.11}$$

The equation (3.11) is a linear system with unique solutions and known as normal equation. By using the equation (3.9), the new residual vector is computed. This is the same as the MP algorithm. All steps are repeated until the current residual norm becomes a very small value approximation to ϵ. The vector *y* will span by a set of active columns in OMP termination. In each iteration, the residual vector *r* in OMP approach is always orthogonal to all active columns. In the next iteration, the correlation of the active columns will be zero. Therefore, the columns are not selected twice. The active set and iteration counter are growing together.

3.2.3 Orthogonal Matching Pursuit with Partially Known Support (OMP-PKS)

The OMP-PKS is a greedy algorithm which is used in the image reconstruction from the measurement vectors *y* and it is derived from the traditional OMP algorithm [64, 65]. OMP-PKS uses the sparse image that has some coefficients more important than the other coefficients. The OMP-PKS approach provides a successful reconstruction to the measurement vector *y* as defined in equations (3.5) and (3.6), where the *M* dimensions of *y* is a very small; that means it has a very low measurement rate *M/N*. The sparse image is generated by using the discrete wavelet transformation DWT [64].

The wavelet transformation in the image shown in the Figure 3.2 is realized by the filter banks.

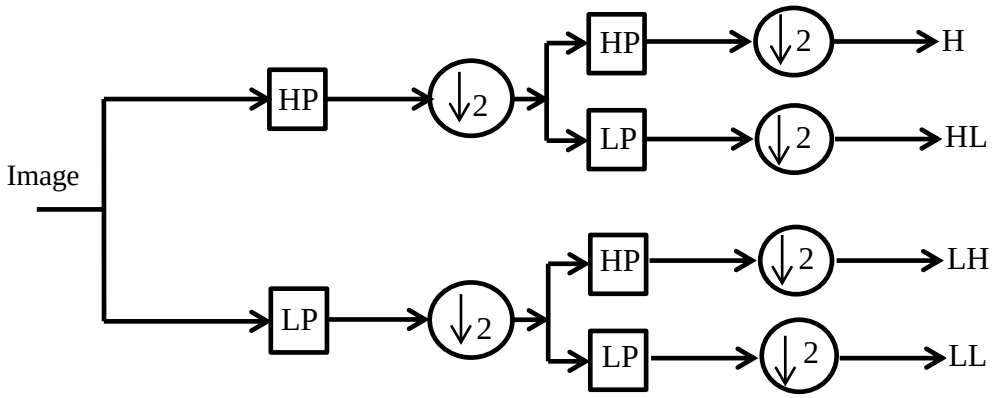

Figure 3.2. Wavelet decomposition by filter bank analysis. HP and LP are high pass filter and low pass filter, respectively [64].

By using the Discrete Wavelet Transformation (DWT), the image decomposes into four sub-bands: approximation sub-band LL, vertical sub-band HL, horizontal sub-band LH and diagonal sub-band HH. The HL, LH and HH sub-bands are called detail sub-band. In this thesis, the DWT has been applied as the octave-tree wavelet transform as depicted in the Figure 3.3, which displays the original and wavelet transformed images. The second level and the third level sub-bands are constructed from the approximation sub-band LL by applying the filter bank analysis. The LL sub-band takes the first and the second levels of DWT.

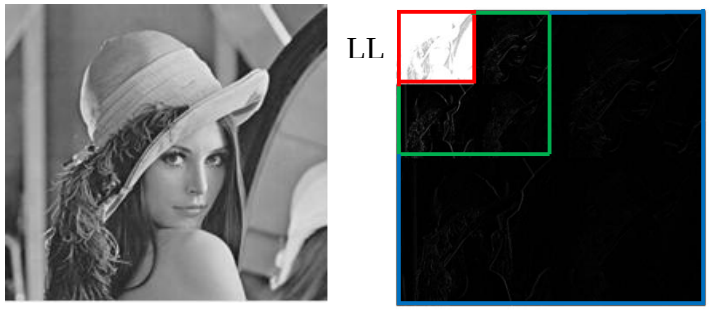

(a) (b)

Figure 3.3. The octave-tree discrete wavelet transform: (a) the original image and (b) the wavelet transformed image. Sub-bands inside the blue, green and red windows are the first, the second and the third level sub-bands, respectively [65].

The LL3 sub-band has been explained in the red region of the Figure 3.4.a; its coefficients have been selected as non-zero elements without testing for correlation. The other colors in the Figure 3.4.a show the detail parts of different DWT levels. The LL3 is a very important sub-band, because it contains most of the energy in the image, this means it has the highest frequencies (large value coefficients). All LL3 sub-band components are used as known support part in the OMP-PKS algorithm. The detail parts are at variance with LL3 part, where the detail parts have lower frequencies (small value coefficients).

Figure 3.4.b shows the rearranging of DWT coefficients, where the LL3 sub-band takes location at the beginning of each row, then it follows by the detail sub-bands of a different DWT levels respectively. The Figure 3.5 depicts the rearranged coefficients that LL3 sub-band takes location in the first four columns. All coefficients of LL3 sub-band are nonzero. Therefore, LL3 sub-band has been used as known support part in this thesis. The sparse image in wavelet domain is divided into blocks along its row as depicted in Figure 3.4.c. These rows in the resulting image are represented as sparse vectors in this thesis. The image can be a sparser image by using the wavelet shrinkage threshold approach [42]. The wavelet shrinkage threshold is used for making most of the coefficients in the detail sub-bands equal to zero, and the other less number of remaining components are nonzero.

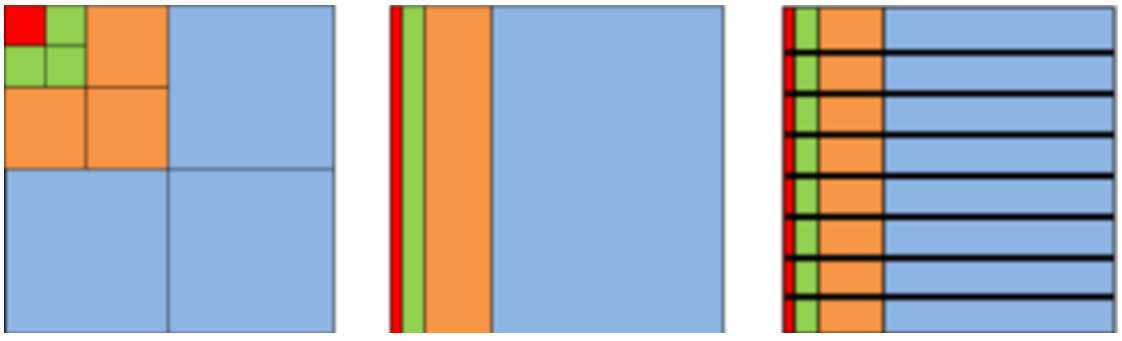

Figure 3.4. Wavelet transform and its block processing: (a) wavelet transformed image, (b) wavelet sub-bands rearranging and (c) wavelet blocks [65].

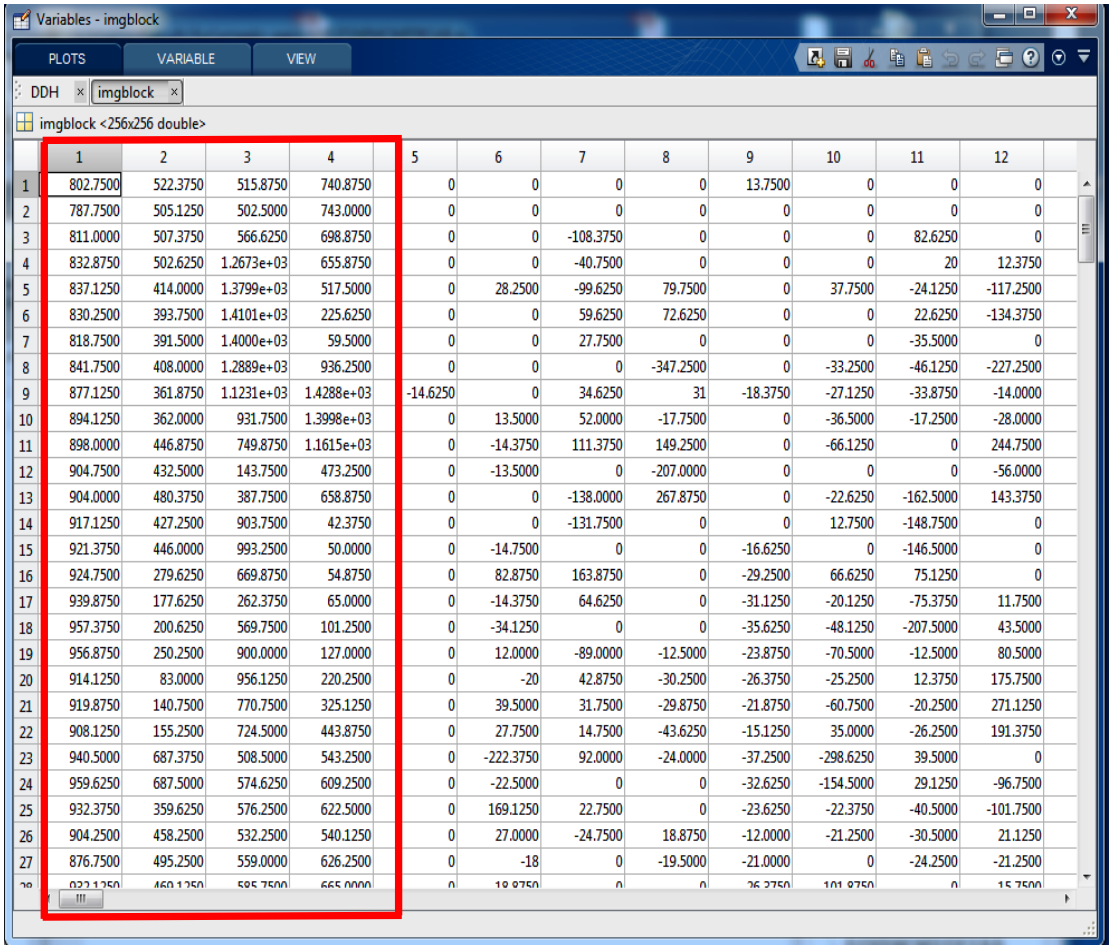

	1	2	3	4	5	6	7	8	9	10	11	12
1	802.7500	522.3750	515.8750	740.8750	0	0	0	0	13.7500	0	0	0
2	787.7500	505.1250	502.5000	743.0000	0	0	0	0	0	0	0	0
3	811.0000	507.3750	566.6250	698.8750	0	0	-108.3750	0	0	0	82.6250	0
4	832.8750	502.6250	1.2673e+03	655.8750	0	0	-40.7500	0	0	0	20	12.3750
5	837.1250	414.0000	1.3799e+03	517.5000	0	28.2500	-99.6250	79.7500	0	37.7500	-24.1250	-117.2500
6	830.2500	393.7500	1.4101e+03	225.6250	0	0	59.6250	72.6250	0	0	22.6250	-134.3750
7	818.7500	391.5000	1.4000e+03	59.5000	0	0	27.7500	0	0	0	-35.5000	0
8	841.7500	408.0000	1.2889e+03	936.2500	0	0	0	-347.2500	0	-33.2500	-46.1250	-227.2500
9	877.1250	361.8750	1.1231e+03	1.4288e+03	-14.6250	0	34.6250	31	-18.3750	-27.1250	-33.8750	-14.0000
10	894.1250	362.0000	931.7500	1.3998e+03	0	13.5000	52.0000	-17.7500	0	-36.5000	-17.2500	-28.0000
11	898.0000	446.8750	749.8750	1.1615e+03	0	-14.3750	111.3750	149.2500	0	-66.1250	0	244.7500
12	904.7500	432.5000	143.7500	473.2500	0	-13.5000	0	-207.0000	0	0	0	-56.0000
13	904.0000	480.3750	387.7500	658.8750	0	0	-138.0000	267.8750	0	-22.6250	-162.5000	143.3750
14	917.1250	427.2500	903.7500	42.3750	0	0	-131.7500	0	0	12.7500	-148.7500	0
15	921.3750	446.0000	993.2500	50.0000	0	-14.7500	0	0	-16.6250	0	-146.5000	0
16	924.7500	279.6250	669.8750	54.8750	0	82.8750	163.8750	0	-29.2500	66.6250	75.1250	0
17	939.8750	177.6250	262.3750	65.0000	0	-14.3750	64.6250	0	-31.1250	-20.1250	-75.3750	11.7500
18	957.3750	200.6250	569.7500	101.2500	0	-34.1250	0	0	-35.6250	-48.1250	-207.5000	43.5000
19	956.8750	250.2500	900.0000	127.0000	0	12.0000	-89.0000	-12.5000	-23.8750	-70.5000	-12.5000	80.5000
20	914.1250	83.0000	956.1250	220.2500	0	-20	42.8750	-30.2500	-26.3750	-25.2500	12.3750	175.7500
21	919.8750	140.7500	770.7500	325.1250	0	39.5000	31.7500	-29.8750	-21.8750	-60.7500	-20.2500	271.1250
22	908.1250	155.2500	724.5000	443.8750	0	27.7500	14.7500	-43.6250	-15.1250	35.0000	-26.2500	191.3750
23	940.5000	687.3750	508.5000	543.2500	0	-222.3750	92.0000	-24.0000	-37.2500	-298.6250	39.5000	0
24	959.6250	687.5000	574.6250	609.2500	0	-22.5000	0	0	-32.6250	-154.5000	29.1250	-96.7500
25	932.3750	359.6250	576.2500	622.5000	0	169.1250	22.7500	0	-23.6250	-22.3750	-40.5000	-101.7500
26	904.2500	458.2500	532.2500	540.1250	0	27.0000	-24.7500	18.8750	-12.0000	-21.2500	-30.5000	21.1250
27	876.7500	495.2500	559.0000	626.2500	0	-18	0	-19.5000	-21.0000	0	-24.2500	-21.2500

Figure 3.5. The coefficients of LL3 sub-band, that are in the first four columns at the red region.

3.3 Digital Watermarking

The watermarking algorithm has been used for information protection [78, 81]. In the communication systems, if there are some important data wanted to be protected, this data is added into the host image before transmitting it. The watermarking algorithm used in this thesis is the same as with the algorithm in [10, 82], but for the reconstruction, we use OMP and OMP-PKS approaches instead of L1 minimization. The watermarking process includes three algorithms: encoder, reconstruction and decoder algorithms:

3.3.1 The encoder algorithm

In the encoder process as explained in the Figure 3.6, a watermark V embeds into the compressive sensed measurements of a sparse signal $x \in R^N$. The watermarking image is represented as $V \in \{-\alpha, +\alpha\}^L$, L is the number of bits in the watermarking image. The measurement vector is symbolized as y_V, where $y_V \in R^M$:

$$y_V = \Phi x + DV. \tag{3.12}$$

where D is a random matrix with M x L, where $L < M \ll N$, and must be known prior to the insertion and extraction procedures. $\Phi \in R^{MxN}$ is a measurement matrix. The watermarked measurements may be changed by parasitical or by channel defects and the decoder receives:

$$y_n = \Phi x + DV. \tag{3.13}$$

That reorders as:

$$y_V = H \begin{bmatrix} x \\ V \end{bmatrix}, \text{ such that } H = [\phi \mid D]. \tag{3.14}$$

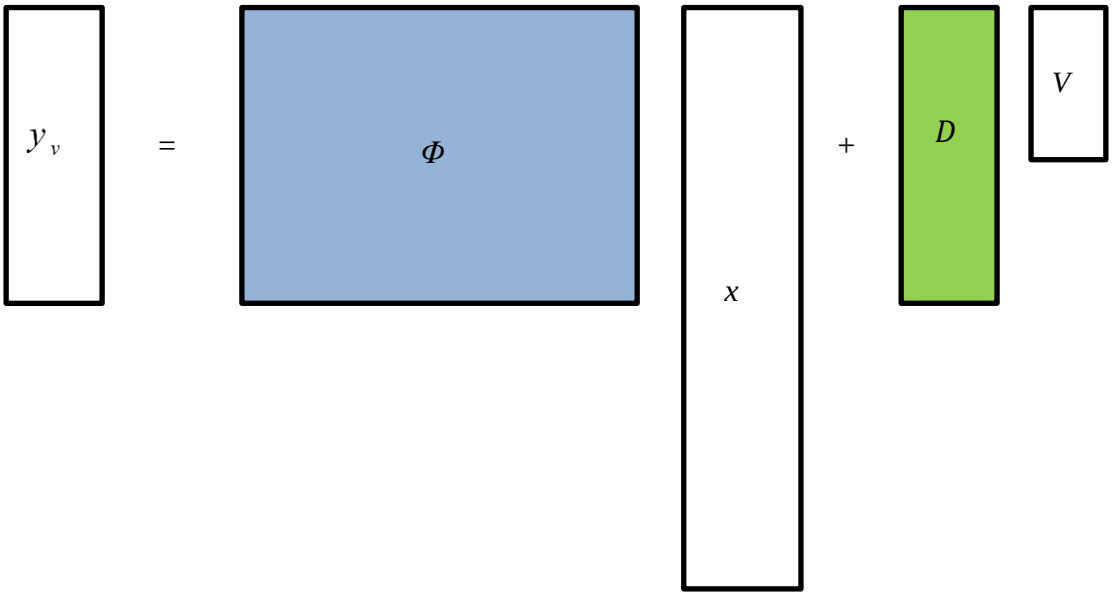

Figure 3.6. Watermarking image embedding structure [10].

3.3.2 The reconstruction algorithms

The three reconstruction algorithms are used to reconstruct the watermarked compressive sensed measurements y_V, the first algorithm is L1 norm minimization algorithm as in [10, 82], which is reconstructed y_V exactly by solving the following equation:

$$\|y - \phi x\|_2. \qquad (3.15)$$

The second reconstruction algorithm is OMP, explained in Table 3.1. Part two and Table 3.2. Part two. The OMP estimates the magnitude of the nonzero coefficients in *x* by solving the least square error between the orthogonal projection of the recovered *x* and measurement vector *y*. The watermarked compressive sensed measurement y_V in equation (3.14) includes both *K*-sparse *x* and *L* bit watermarking image *V*.

$$\hat{x} = \arg\min_x \|y - \phi x\|_2.$$

Then It is changed as:

$$\hat{Z} = argmin_x \ ||y_V - HZ||_2. \qquad (3.16)$$

Where: $\hat{Z} = \begin{bmatrix} \tilde{x} \\ \tilde{v} \end{bmatrix}, Z = \begin{bmatrix} x \\ V \end{bmatrix}$ *and* $H = [\phi | D]$.

The third reconstruction algorithm is OMP-PKS, which is successfully reconstructed y_V. Let *T* is a set that includes indexes of the LL3 sub-band coefficients as explained in the Figure 3.5, which is represented the known support part that all components in it are nonzero.

$$T = \text{(index of known port)}, T = \{\gamma_1, \gamma_1, \ldots, \gamma_{|T|}\}. \qquad (3.17)$$

The procedure of OMP-PKS algorithm is divided into two parts detailed in the Table 3.1 and Table 3.2, the first part uses the partially known support PKS that provides a priori knowledge to compute the important sub-bands in the sparse image. The second part shows the OMP algorithm.

3.3.3 The decoder algorithm

The decoder procedure is used for the watermarking image extraction. After reconstructing the watermarked compressive sensing measurements y_V, the watermarking extraction is used to extract the watermarking image as in [10]. The decoder procedure utilizes two methods to detect the watermarking image. In the first method, the watermarking image is extracted from the reconstructed watermarked measurement vectors, i.e. it is reconstructed by using the L1-min, OMP and OMP-PKS algorithms. When the L1-min uses as reconstruction algorithm, the watermarking and recovered images are represented as:

$$\begin{bmatrix} \tilde{x} \\ \tilde{V} \end{bmatrix} = \min_{[x \quad V]'} \left\| \begin{bmatrix} x \\ V \end{bmatrix} \right\|_{l_1} .$$

$$\hat{V} = \alpha \; sgn\,(\tilde{V}). \tag{3.18}$$

$$\hat{x} = min_x \; \|x\|_{l_1} \text{ Subject to } \left\|(y_V - D\hat{V}) - \phi x\right\|_{l_2} . \tag{3.19}$$

where $\hat{V}$ is the extracted watermark image and $\hat{x}$ is the recovered image. The watermarking image is extracted from the reconstructed watermarked compressive sensed vectors which use the OMP in the reconstruction as shown in Table 3.1. Part two where:

$$\hat{Z} = argmin_x \; \|y_V - HZ\|_2 .$$

$$\begin{bmatrix} \tilde{x} \\ \tilde{v} \end{bmatrix} = \hat{Z} .$$

$$\hat{V} = \alpha * sgn\,(\tilde{V}_i).$$

where $\hat{V}$ is the extracted watermark image and $\hat{x}$ is the recovered image after solving the least square error problem of the equation (3.19). Also, the watermarking image is extracted as in Table 3.1 from the reconstructed watermarked measurements that use the

OMP-PKS as reconstruction algorithm. The OMP-PKS algorithm has indexes of the known support part coefficients as defined in the following equation:

$$Z_{t^K} = (H' \ H)^{-1} \ H' \ y_V \qquad (3.20)$$

Table 3.1. OMP-PKS and OMP algorithms in the first decoder method

Inputs:	$H = [\Phi \mid D]$: measurement (sensing) matrix. y_V: watermarked measurement vector by Mx1. $\lambda_0 = \{\}$ index set of support of x. V: watermarked image, $V \in \{-\alpha, +\alpha\}^L$. L is the number of bits. T: known support part. K: Sparsity rate.
Procedure	
Part one	
Initialize:	$t^K = \lvert T \rvert$, iteration T = (index of known support part, $T = \{\gamma_1, \gamma_1, \ldots, \gamma_{\lvert T \rvert}\}$. $\Lambda = T$. $Z = \begin{bmatrix} x \\ V \end{bmatrix}$. $H = [\varphi_{\gamma_1}, \varphi_{\gamma_2}, \varphi_{\gamma_3}, \ldots, \varphi_{\gamma_{t^K}}]$, $Z_{t^K} = (H' \ H)^{-1} \ H' \ y_V$. $a_{t^K} = \langle HZ \rangle$. $r = y_V - H_T \ (H_T^{\dagger} \ y)$. Or $r = y_V - a_{t^K}$
Part two	
While	$t << K$. $t = t+1$. $G_t = \text{argmax}_{j=[1\ N], j \notin \Lambda_{t-1}} \lvert < r_{t-1} \ H_j > \rvert$. $\Lambda_t = \Lambda_{t-1} \cup \ G_t$. $H_t = \{ H_{t-1} \cup \ G_t \}$. $Z_t = arg \ min_x \left\lVert y - H_{\lambda_t} Z \right\rVert_2$. $a_t = < H_t \ Z_t >$. $r_t = y - a_t$.

End
Outputs: $\hat{Z} = argmin_x \left\| y_V - H_{\lambda_t} Z \right\|_2$. $\begin{bmatrix} \tilde{x} \\ \tilde{V} \end{bmatrix} = \hat{Z}$. $\hat{V} = \alpha * sgn(\tilde{V}_i)$. $\hat{x} = \arg\min_x \left\| (y_V - D\hat{V}) - \phi x \right\|_2$ $\Lambda_K = \{\lambda_n\}$, $n = 1, 2, \ldots, K$.

In the second decoder method, the new matrix Q is created, where $Q \in R^{MxN}$ is a random matrix, and D matrix represents a null space of the matrix Q. Then the matrix Q will eliminate the matrix D, $QD = 0$. The important point in this system is that the matrices QD must satisfy the RIP of order $2K$. Then y_V in the equation (3.12) is expressed as follows:

$$\tilde{y} = Q(\Phi x + DV) = Q\Phi x, \; QDV = 0. \tag{3.21}$$

The reconstructed watermarked compressive sensed vector by using L1 norm minimization is expressed in the following equation:

$$\hat{x} = min_x \left\| x \right\|_{l_1} \text{ Subject to } \left\| \tilde{y} - Q\phi x \right\|_{l_2}. \tag{3.22}$$

where $\hat{x}$ is the recovered image, then the watermarking image is extracted by using the following equation:

$$\tilde{V} = (D^T D)^{-1} D^T (y_V - \Phi\hat{x}). \tag{3.23}$$

After finding $\tilde{V}$, the equation (3.18) is used for computing the finally watermarking image extraction. By using the OMP algorithm, shown in Table 3.2 (part two) and OMP-PKS algorithm, shown in Table 3.2 (part one) are used to reconstruct the watermarked measurements, then the exact watermarking image extraction and recovered image are shown as:

$$\hat{x} = argmin_x \ \|y - \phi x\|_2, \ \tilde{V} = (D' D)^{-1} D' (y_V - \Phi\hat{x}).$$

After $\tilde{V}$ is computed, the decoder uses the equation (3.18) to extract the watermarking image.

Table 3.2. OMP-PKS and OMP algorithms in the second decoder method

Inputs:	Φ: measurement (sensing) matrix by MxN. y_V: watermarked measurement vector by Mx1. $\tilde{y} = Q\Phi x$: measurement vector by Mx1. λ_0= {} index set of support of x. V: watermarked image, $V \in \{-\alpha, +\alpha\}^L$. L is the number of bits. T: known support part. K: Sparsity rate.
Procedure	
	Part one
Initialize:	t^K=|T|, iteration. T = (index of known support part), $T = \{\gamma_1, \gamma_1, \ldots, \gamma_{\|T\|}\}$. $\Lambda = T$. $\Phi = [\ \varphi_{\gamma_1}, \varphi_{\gamma_2}, \varphi_{\gamma_3}, \ldots, \varphi_{\gamma_{t^K}}\ ]$. $x_{t^K} = (\Phi' \ \Phi)^{-1} \ \Phi' \ \tilde{y}$. $a_{t^K} = <\Phi \ x_{t^K} >$. $r = y - \Phi_T (\Phi_T^{\dagger} \tilde{y})$. O $r = \tilde{y} - a_{t^K}$.
	Part two
While	$t << K$. $t = t+1$. $G_t = \text{argmax}_{j=[1\ N], j \notin \Lambda_{t-1}} \| < r_{t-1} \ \Phi_j > \|$. $\Lambda_t = \Lambda_{t-1} \cup \ G_t$. $\Phi_t = \{\ \Phi_{t-1} \cup \ G_t\ \}$. $x_t = \arg min_x \ \|y - \Phi_{\lambda_t} x\|_2$. $a_t = <\Phi_t \ x_t >$. $r_t = y - a_t$.
End	
Outputs:	$\hat{x} = argmin_x \ \| y - \Phi x \|_2$. $\tilde{V} = (D' D)^{-1} D' (y_V - \Phi\hat{x})$. $\hat{V} = \alpha$ *sgn ($\tilde{V}_i$).

$$\Lambda_k = \{\lambda_n\},\ n = 1, 2, \ldots, K.$$

3.4 Proposed Flowchart

In this section, we display a proposed flowchart to integrate all the previously explained algorithms (encoder method, reconstruction algorithms and decoder method) and all procedures of this thesis. This flowchart is depicted as follows:

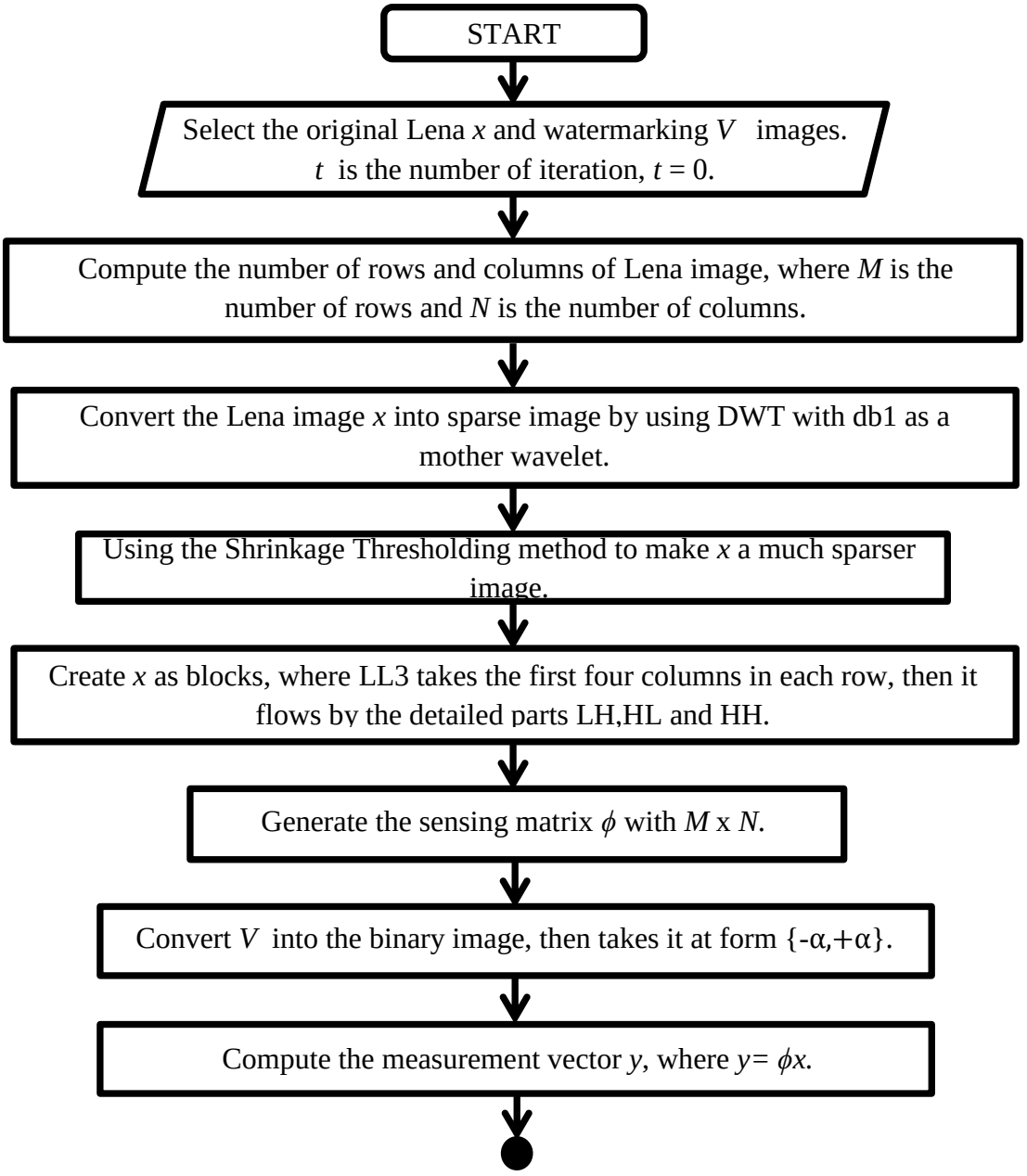

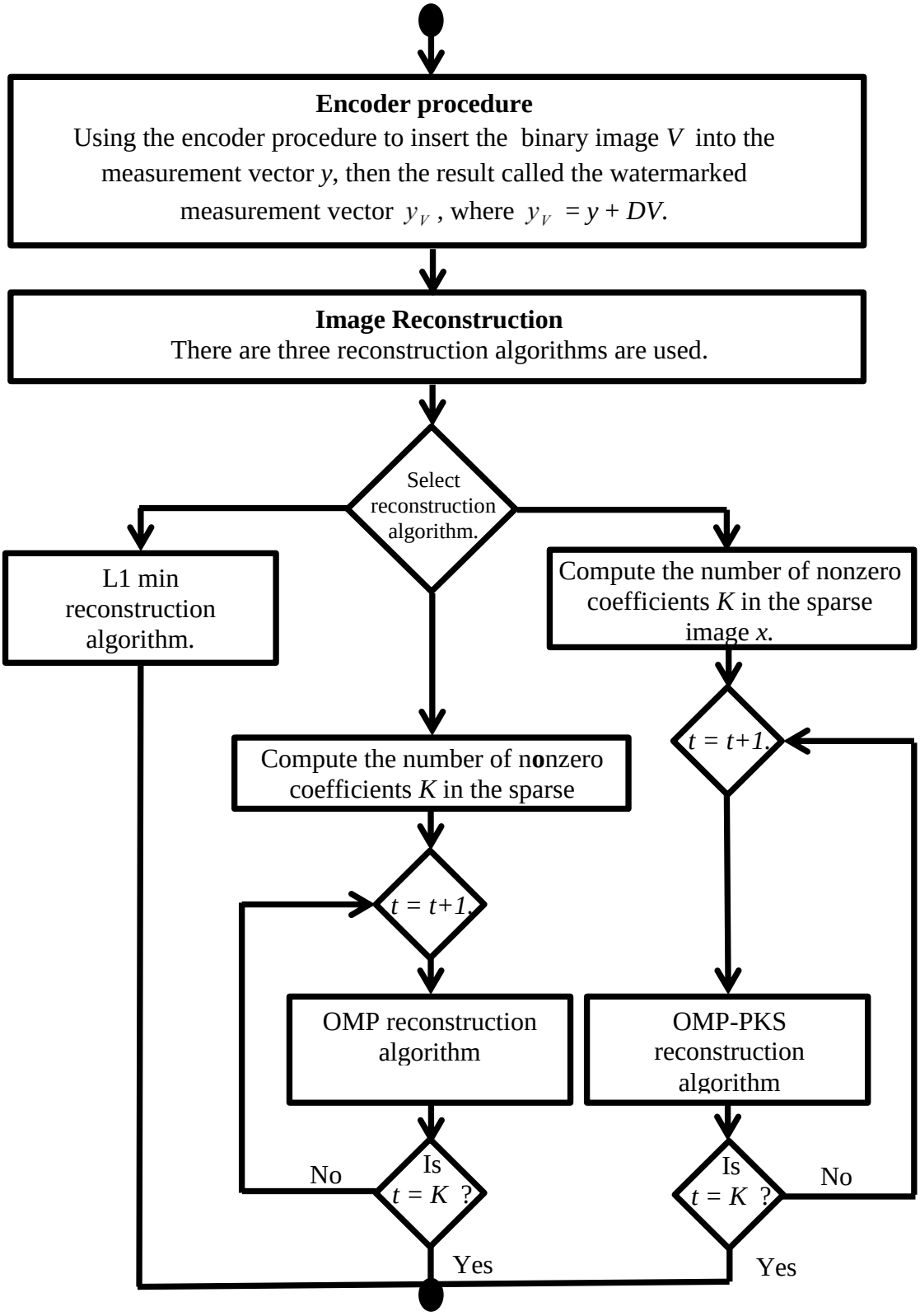
Encoder procedure
Using the encoder procedure to insert the binary image V into the measurement vector y, then the result called the watermarked measurement vector y_V, where $y_V = y + DV$.
Image Reconstruction
There are three reconstruction algorithms are used.
Select reconstruction algorithm.
L1 min reconstruction algorithm.
Compute the number of nonzero coefficients K in the sparse image x.
t = t+1.
Compute the number of nonzero coefficients K in the sparse
t = t+1.
OMP reconstruction algorithm
OMP-PKS reconstruction algorithm
Is t = K ?
No
Yes
Is t = K ?
No
Yes

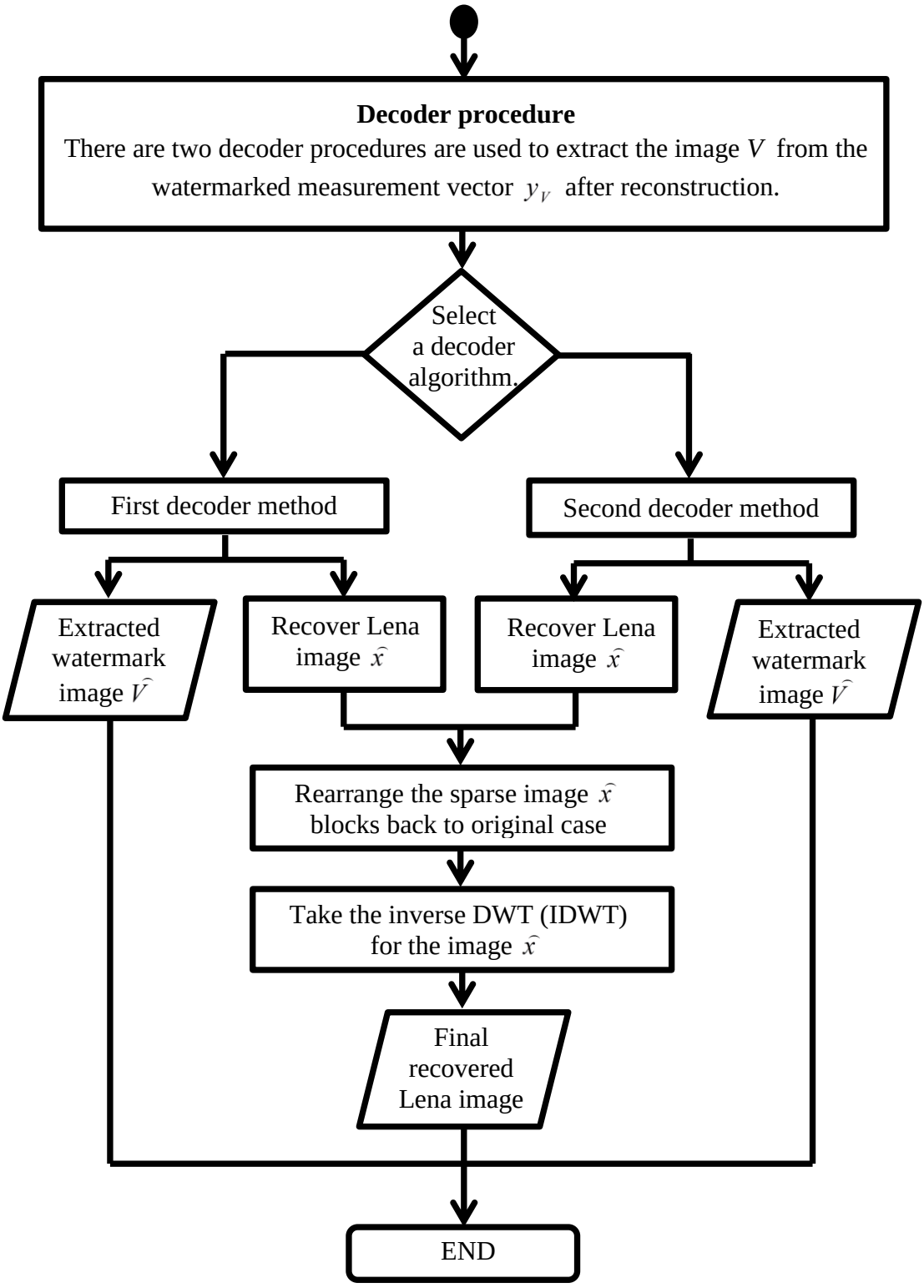

Figure 3.7. The proposed flowchart.

CHAPTER 4

RESULTS AND DISCUSSION

This chapter discusses and displays all experimental results in this thesis. These results are implemented by using a PC with processor Intel (R) Core (TM) i5-2430M, CPU 2.40GHz, and 6 GB of RAM. All algorithms and programs are executed using 46 bits R2013a Matlab program. The original Lena and the watermarking image have 256x256 and 64x64 sizes respectively as depicted in Figure 4.1. The DWT is used to convert the original image into a sparse image by the octave transformation. The Daubechies 1 (db1) is used as a mother wavelet. In addition, the shrinkage hard thresholding is also used to make the image much sparser.

After DWT implementation for the original image, the resulting image is divided into 256 blocks and each block consists of 1x256 row vector. These vectors are used as sparse vectors in this thesis. The measurement matrix Φ has been created by random Gaussian distribution as shown in Figure 4.2.a, which is satisfying RIP in order K with an interval which varies between -0.252 to 0.246. There are two other matrices D and Q generated also by using a random Gaussian. The details has been used of D and Q matrices are explained in the previous chapter (Methodology). The matrix Q has been used to eliminate the matrix D in the watermarking extraction procedure, where DQ =0. The important point is ΦQ which must satisfy RIP as shown in Figure 4.2.b through an interval which varies between -0.226 to 0.265.

a b

Figure 4.1. (a) Original Lena image and (b) Watermarking image.

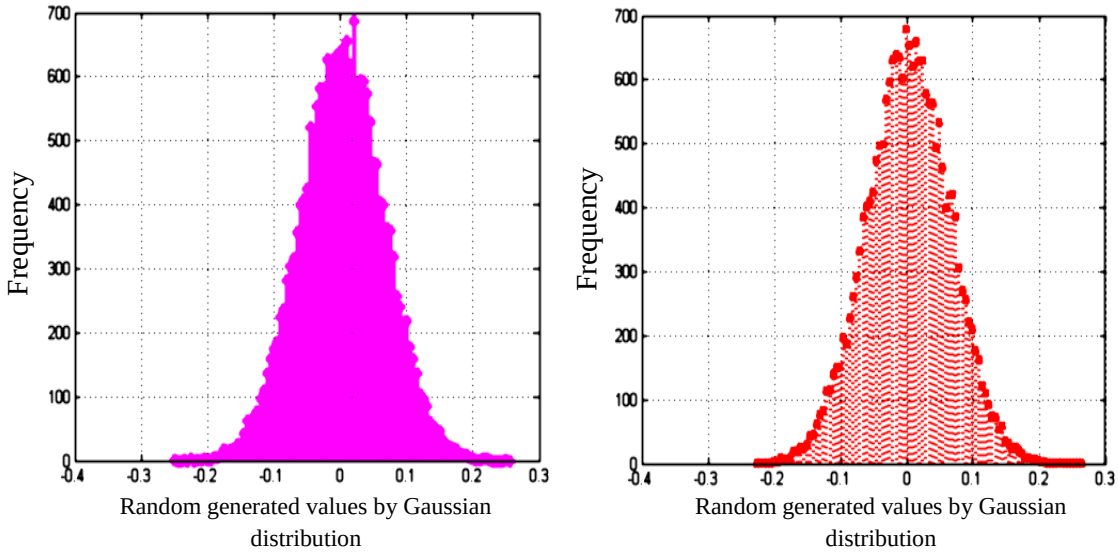

Figure 4.2. (a) Random Gaussian distribution of the sensing matrix Φ. (b) Random Gaussian distribution of ΦQ matrices.

The watermarking image is embedded into the compressive sensing measurements by using the encoder procedure. The resulting watermarked measurements are reconstructed by using three reconstruction algorithms L1-min, OMP and OMP-PKS. The L1-min algorithm reconstructs the watermarked measurements. The performance of L1 algorithm has been tested by using a wide interval of the measurement rates *M/N* that are taken between 0.234 to 0.840 and the peak signal to noise ratio PSNR computes in each value of *M/N* with its execution time as shown in Table 4.1.

The Figure 4.3 shows the reconstructed Lena image by L1-min and the extracted watermarking image in the first decoder method, where the exact reconstruction of Lena image and the accuracy extraction of watermarking image obtain when *M/N*= 0.762 with maximum PSNR= 29.885. Other high *M/N* values give the same PSNR and same quality of the resulting images. But in the second decoder method, the reconstructed image by L1-min and the extracted watermarking image do not have a good quality in the maximum measurement rate *M/N*= 0.840 with maximum PSNR =29.885. Therefore, the L1-min algorithm does not have a good performance compared to the other two reconstruction algorithms in the second decoder approach.

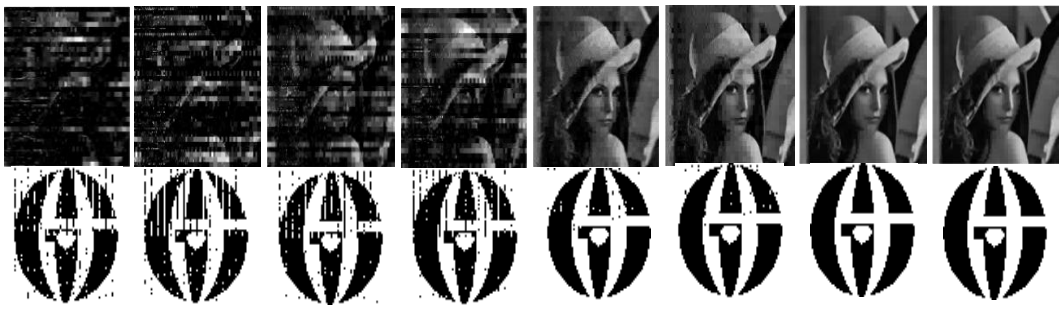

M/N:	0.234	0.254	0.313	0.332	0.352	0.742	0.762	0.840
PSNR:	10.415	10.422	12.78	13.062	14.074	29.885	29.885	29.885

Figure 4.3. The quality of the reconstructed image with the extracted watermarking image in varying *M/N* rates using L1-min in the first decoder method.

M/N:	0.234	0.254	0.313	0.332	0.352	0.723	0.742	0.840
PSNR:	10.415	10.422	12.78	13.062	14.074	29.885	29.885	29.885

Figure 4.4. The quality of the reconstructed image with the extracted watermarking image in varying *M/N* rates using L1-min in the second decoder method.

In the case of the OMP approach for reconstruction the watermarked measurements in the first decoder method, the reconstructed image and extracted watermark image have a better quality in case *M/N*= 0.547 with maximum PSNR= 29.885 as depicted in Figure 4.5. But in the second decoder method, in case *M/N*= 0.840 the maximum PSNR= 29.885, the extracted watermarking image does not have a good quality as shown in Figure 4.6.

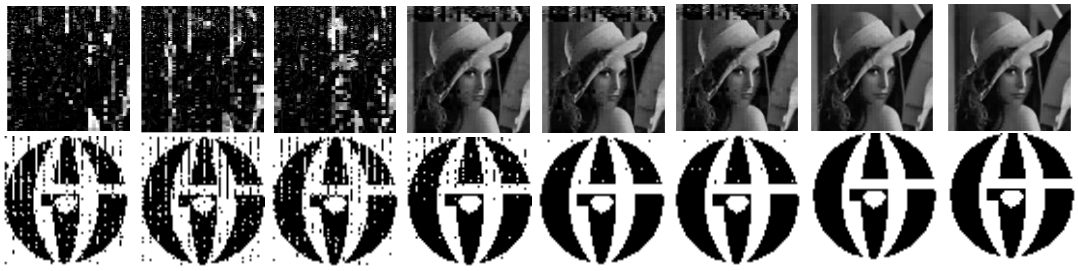

M/N: 0.234	0.254	0.273	0.332	0.352	0.527	0.547	0.840
PSNR: 8.136	7.978	8.264	9.77	10.363	29.885	29.885	29.885

Figure 4.5. The quality of the reconstructed image with the extracted watermarking image in varying *M/N* rates using the OMP algorithm in the first decoder method.

M/N:0.234	0.254	0.273	0.332	0.352	0.703	0.723	0.840
PSNR:29.776	29.782	29.796	29.853	29.856	29.884	29.884	29.884

Figure 4.6. The quality of the reconstructed image with the extracted watermarking image in varying *M/N* rates using the OMP algorithm in the second decoder method.

The OMP-PKS algorithm is also used to reconstruct the watermarked measurements. In the first decoder approach, the reconstructed image by OMP-PKS and the extracted watermarking image have a good quality in small values of the measurement rate *M/N* compared with the other previous reconstruction approaches, where *M/N*= 0.313 the maximum PSNR becomes 37.991 and the higher *M/N* values get the same PSNR as shown in Figure 4.7. In the second decoder method, the extracted watermark image has also a high quality when M/N=0.313 with maximum PSNR value 37.991 as depicted in Figure 4.8.

M/N: 0.234	0.254	0.313	0.332	0.352	0.371	0.820	0.840
PSNR:14.739	20.044	37.991	37.991	37.991	37.991	37.991	37.991

Figure 4.7. The quality of the reconstructed image with the extracted watermarking image in varying *M/N* rates using the OMP-PKS algorithm in the first decoder method.

M/N: 0.234	0.254	0.313	0.332	0.352	0.371	0.391	0.840
PSNR:37.47	37.694	37.991	37.991	37.991	37.991	37.991	37.991

Figure 4.8. The quality of the reconstructed image with the extracted watermarking image in varying *M/N* rates using the OMP-PKS algorithm in the second decoder method.

The Table 4.1 shows the different values of measurement rates *M/N* and in each of *M/N* the PSNR value is computed with its execution time at sec. The Figure 4.9 shows a various values of mean square error MSE, residual *r* and PSNR with different measurement rates *M/N* at both of the two decoder methods. This figure also shows the three reconstruction algorithms L1-min, OMP and OMP-PKS together to explain the performance of these algorithms. The OMP-PKS uses a small measurement rate *M/N* to produce a high efficiency and a better quality of the reconstructed image together with

the extracted watermark image by using both the first and the second decoder algorithms. Also the OMP-PKS algorithm has a high PSNR value in varying *M/N* rates than the other approaches. Therefore, the OMP-PKS algorithm has a high efficiency and better performance in the sparse image reconstruction than the other two reconstruction algorithms.

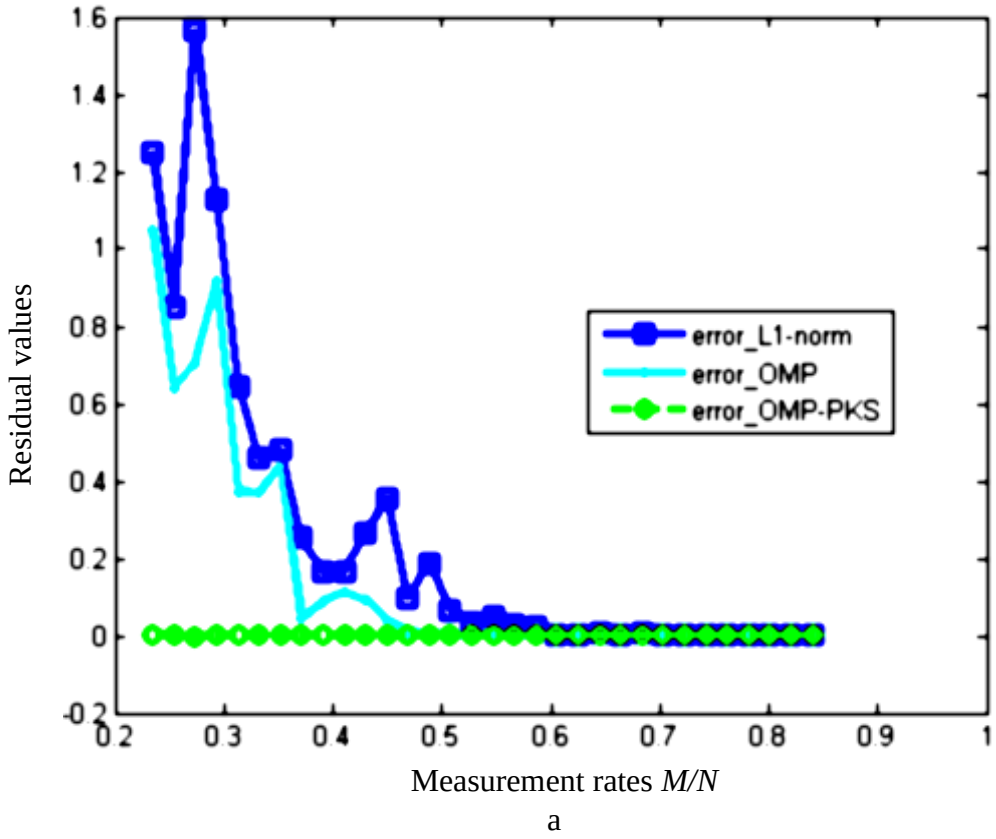

a

Figure 4.9. (a) Residual values with different *M/N* in the first decoder method.

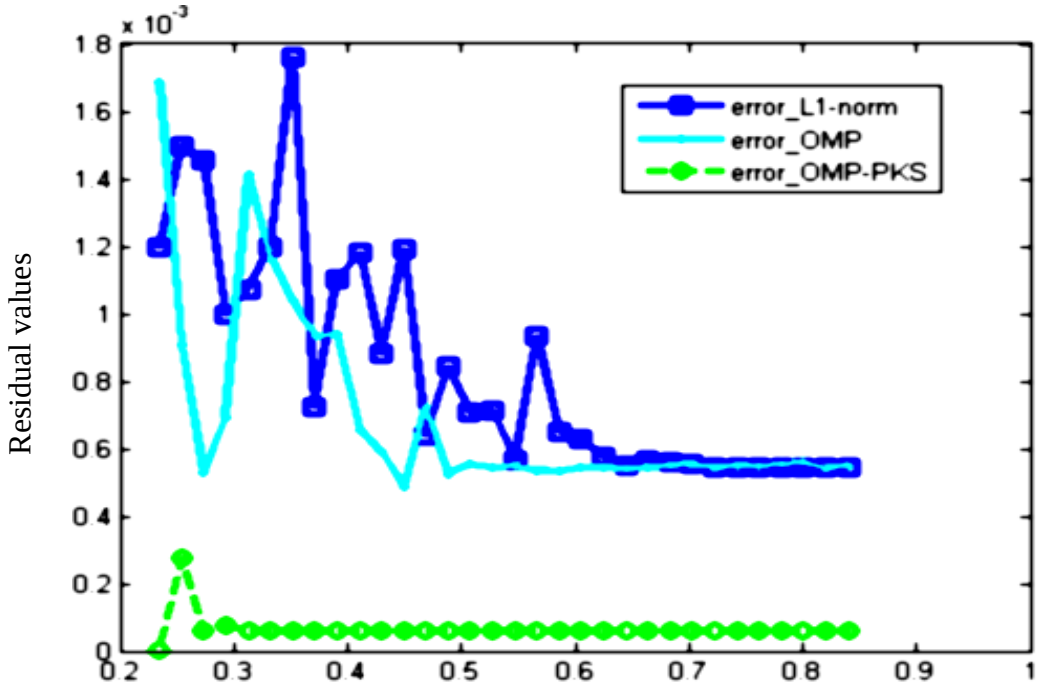

b

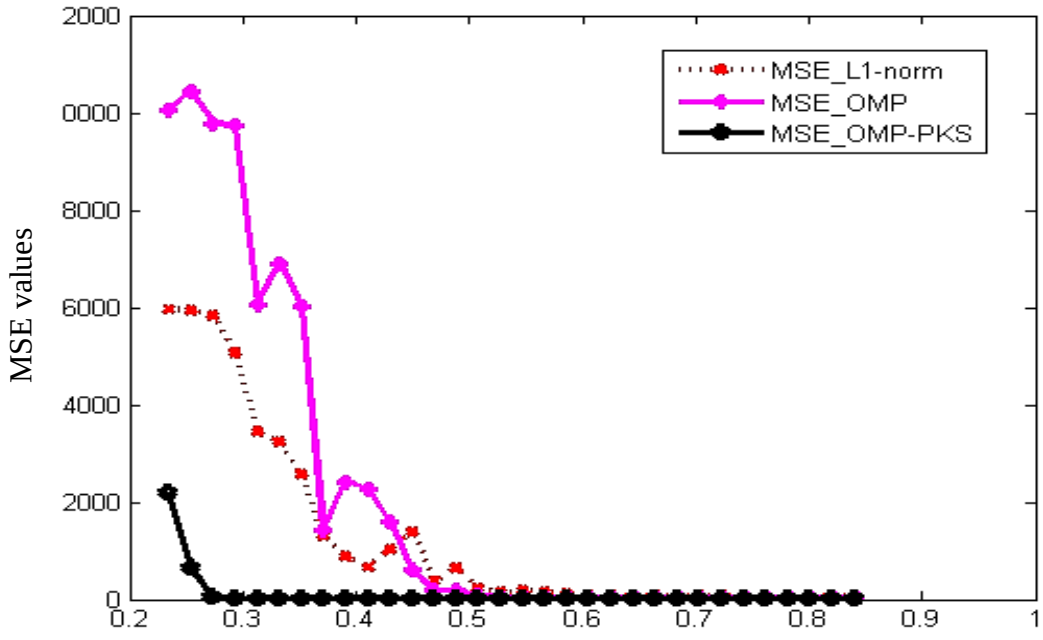

c

Figure 4.9. (b) Residual values with varying *M/N* in the second decoder method. (c) MSE values with varying *M/N* in the first decoder method.

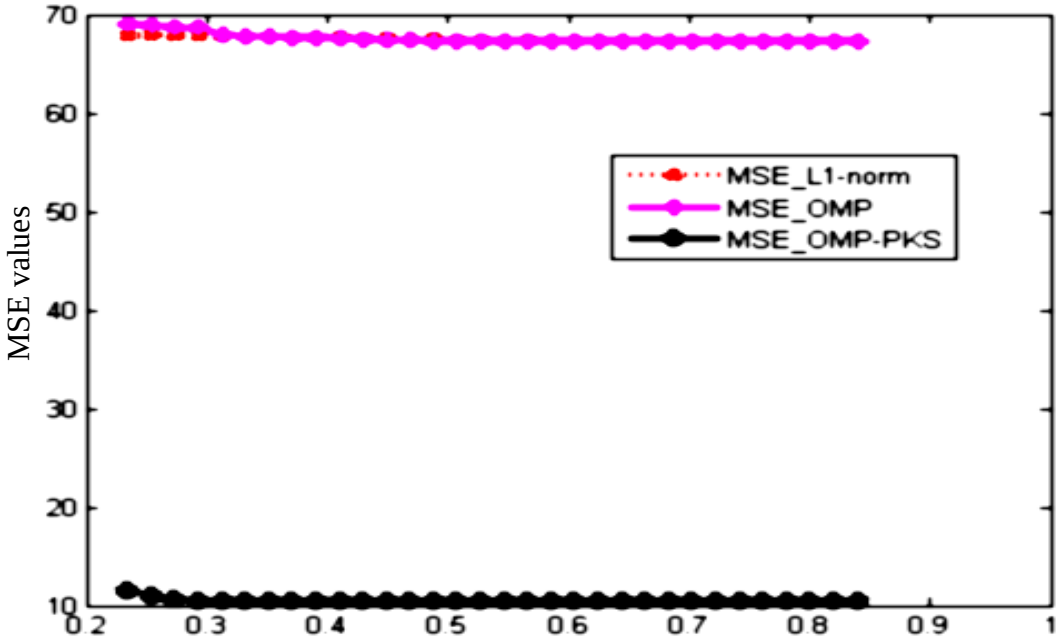

d

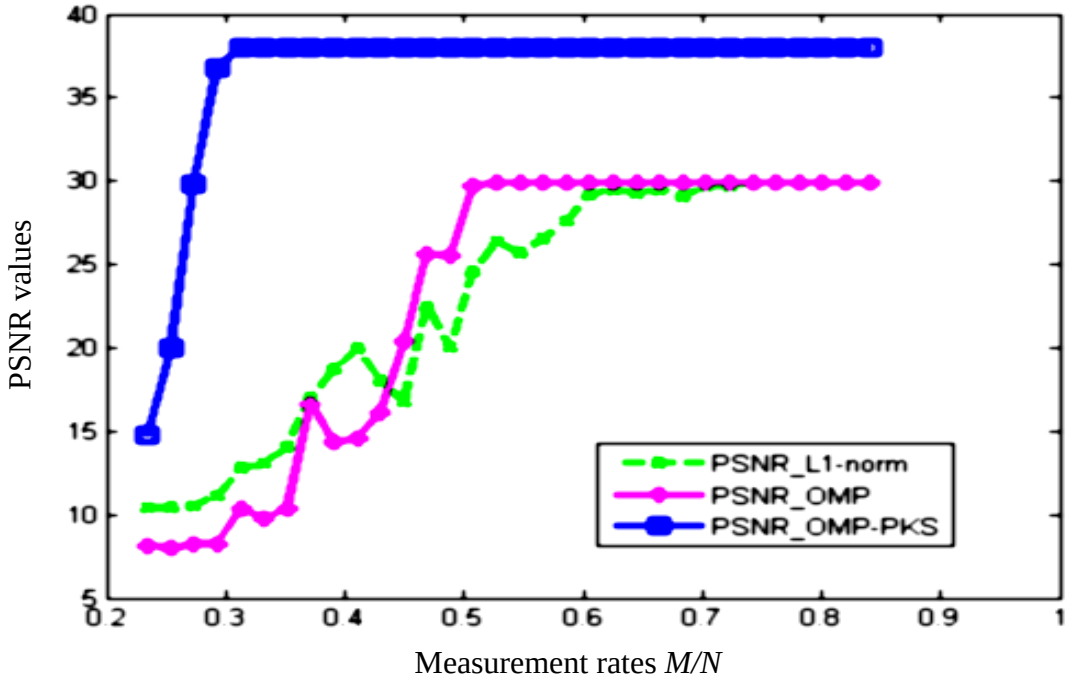

e

Figure 4.9. (d) MSE values with different *M/N* in the second decoder method. (e) PSNR values with varying *M/N* in the first decoder method.

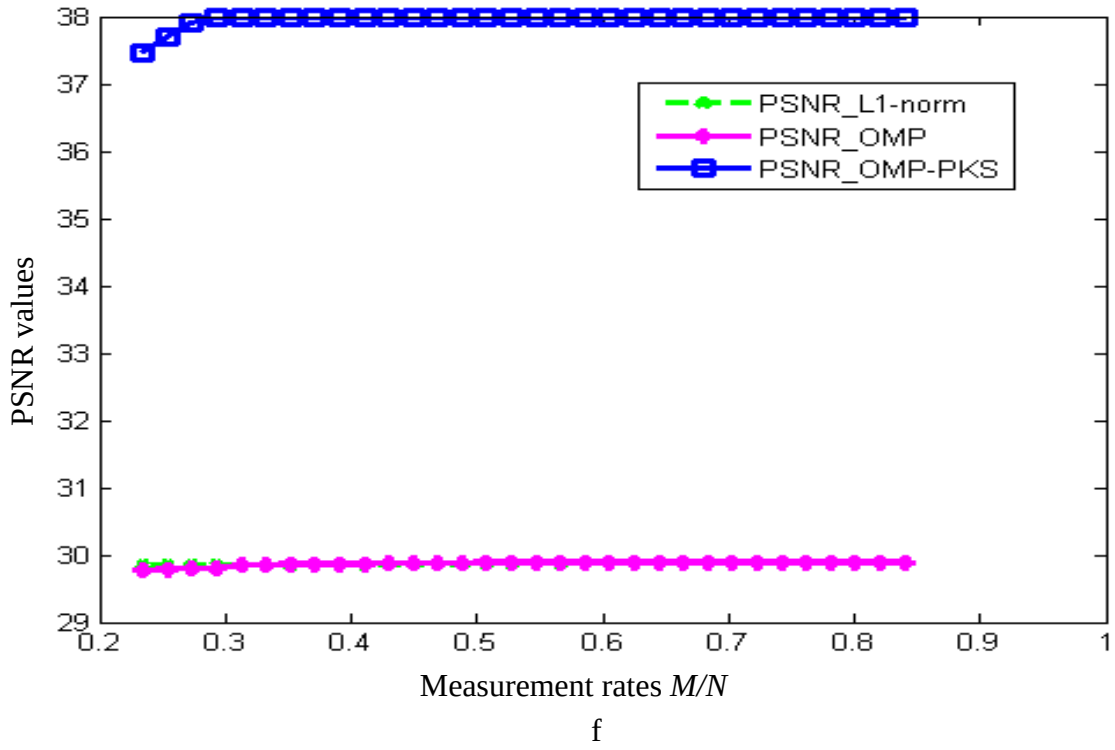

f

Figure 4.9. (f) PSNR values with different *M/N* in second decoder method.

In addition, the nonzero coefficients *K* in the sparse image are taken as varying *K* values to study the performance of the reconstruction algorithms. When the Sparsity rates *K/N* take on various values ranging from 21.508 to 45.648, then in each Sparsity rate *K/N* the PSNR is evaluated. Thus, there are different sets of the PSNR values according to the three different reconstruction methods. The Table 4.2 shows the varying *K/N* rates with different PSNR values and the execution time. Then both the first and the second decoder methods are utilized to extract the watermarking image after each reconstruction for the watermarked measurement vectors by using each of the three reconstruction approaches. Also the residual *r*, MSE and the PSNR values are evaluated by taking varying rates of *K/N* as depicted in Figure 4.10 to explain performance of the reconstruction algorithms. All results show high performance and faster implementation of the OMP-PKS algorithm than the other reconstruction algorithms.

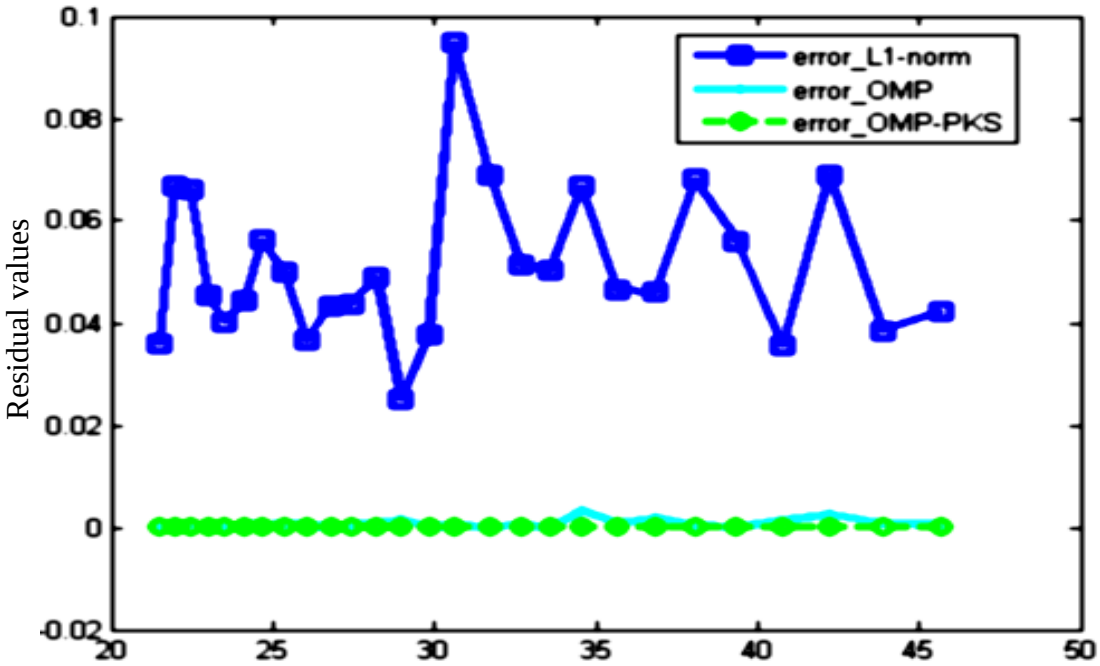

Different Sparsity rates *K/N*

a

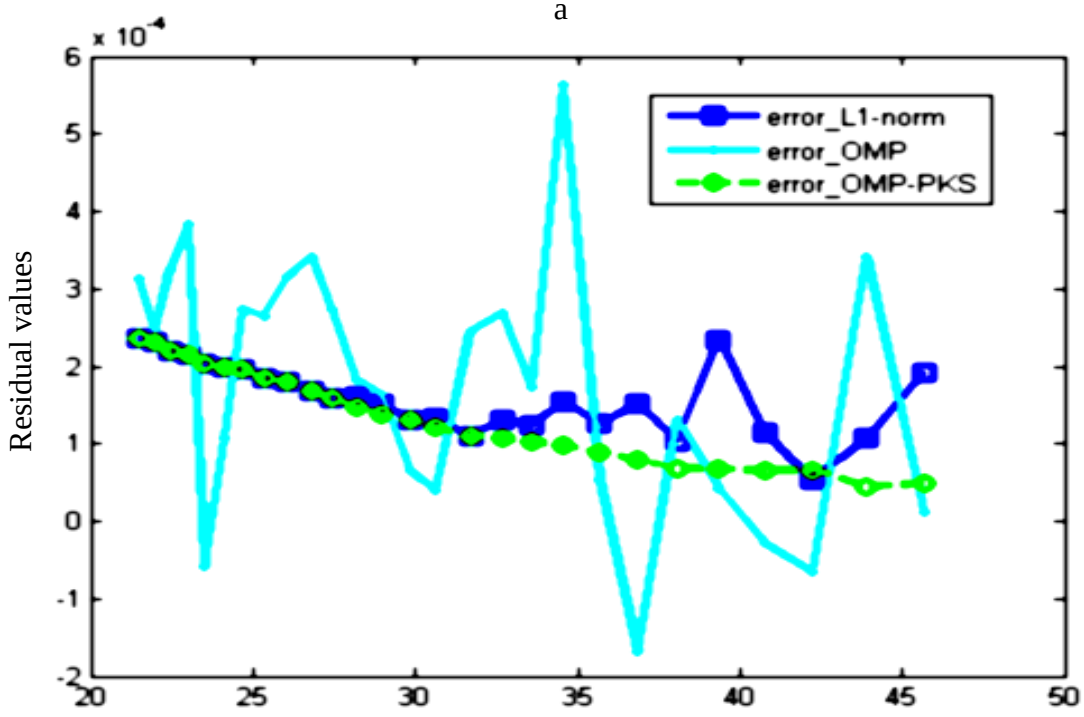

Different Sparsity rates *K/N*

b

Figure 4.10. Performance of the L1-min, OMP and OMP-PKS algorithms in varying *K/N* values, (a) Residual with different *K/N* values in the first decoder method. (b) Residual with different *K/N* values in the second decoder method.

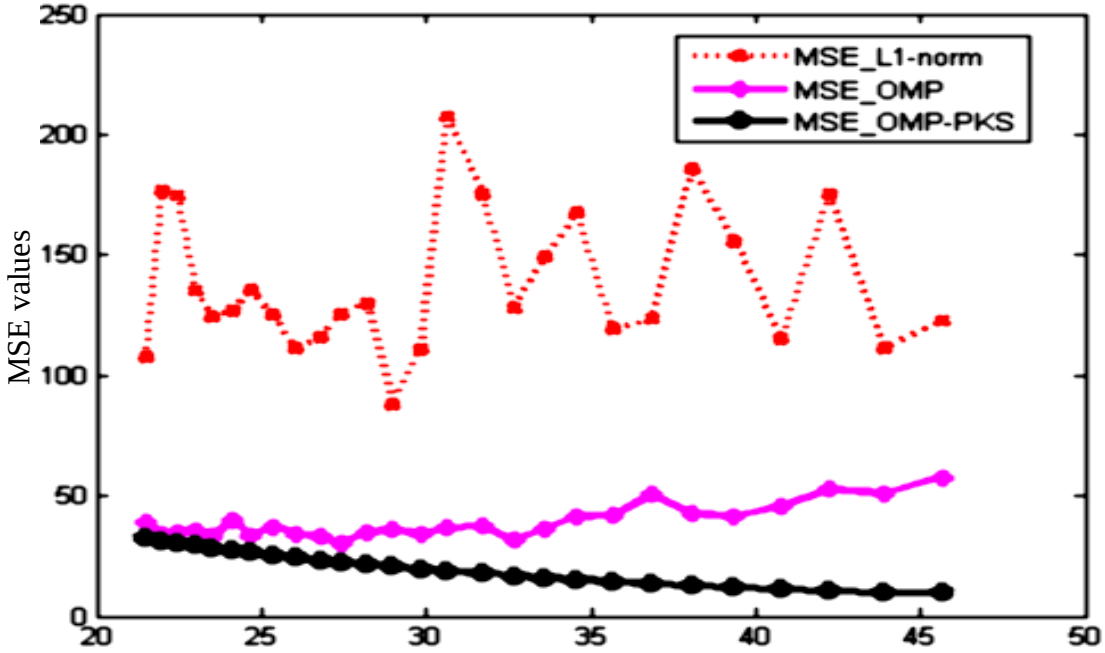

c

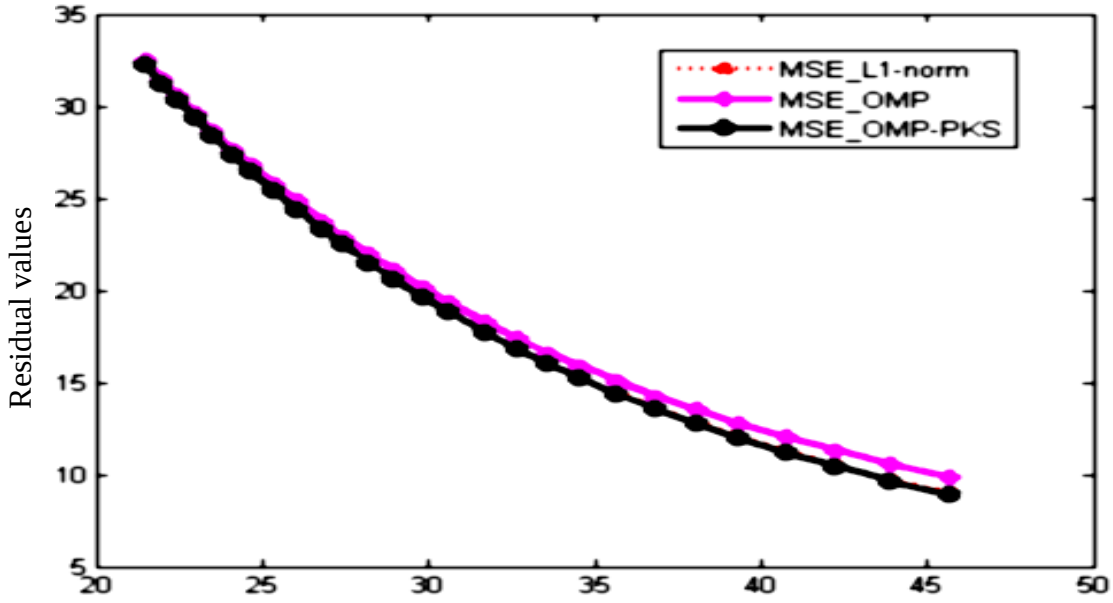

d

Figure 4.10. Performance of the L1-min, OMP and OMP-PKS algorithms in varying *K/N* values, (c) MSE with different *K/N* values in the first decoder method. (d) MSE with different *K/N* values in the second decoder method.

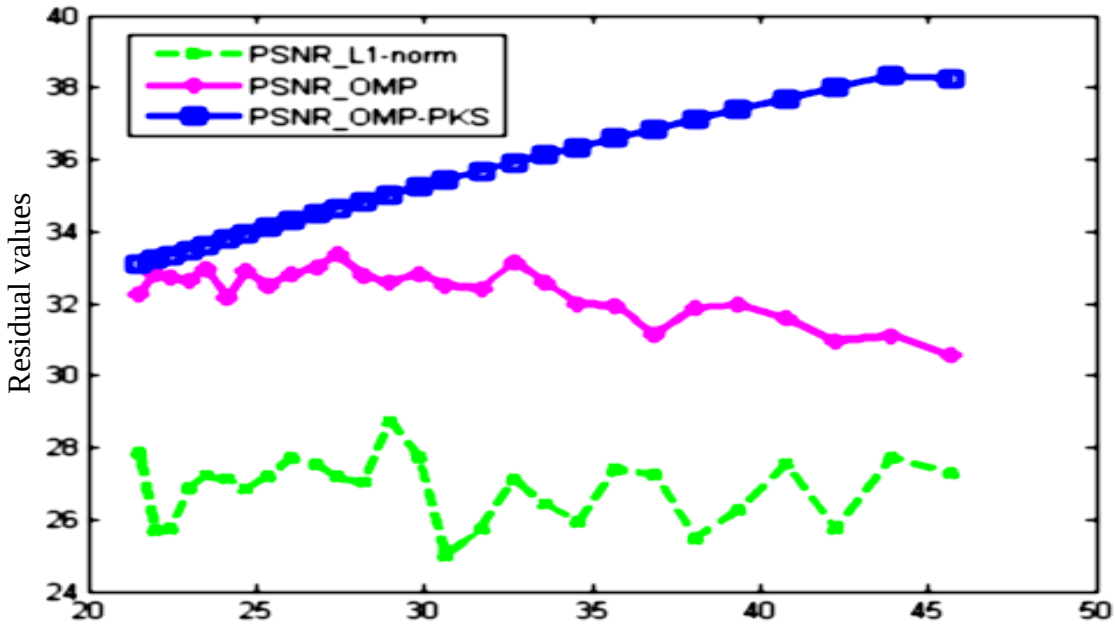

e

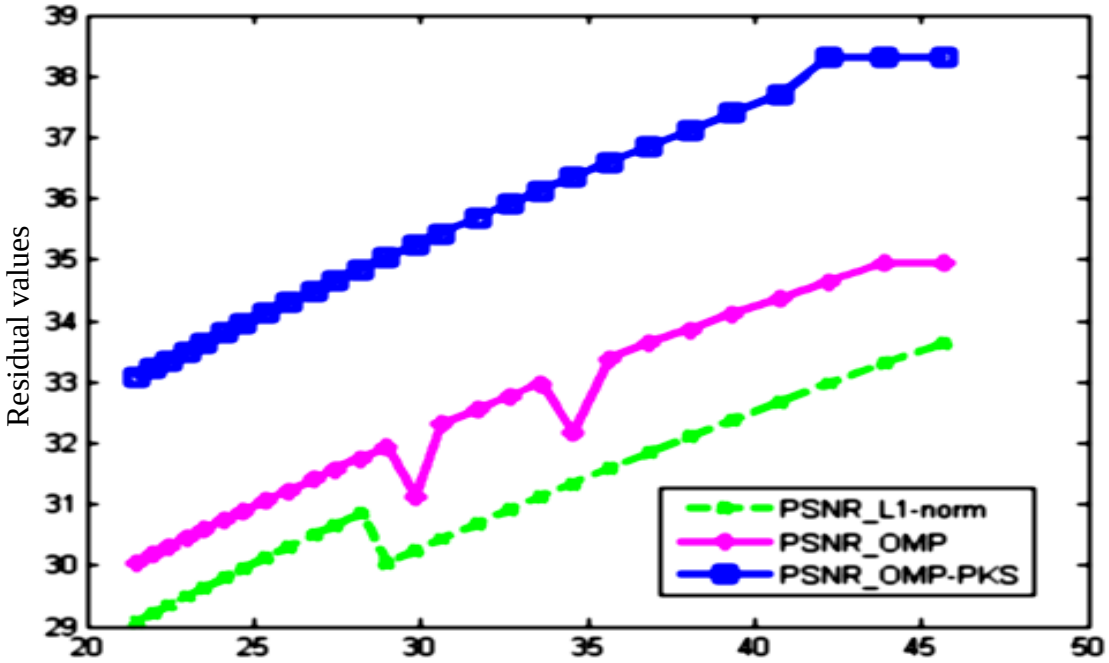

f

Figure 4.10. Performance of the L1-min, OMP and OMP-PKS algorithms in varying *K/N* values, (e) PSNR with different *K/N* values in the first decoder method. (f) PSNR with different *K/N* values in the second decoder method.

Table 4.1. PSNR and its execution time with different measurement rates *M/N* by using the three reconstruction algorithms with the first and second decoder methods.

Measurement rates		L1-min algorithm				OMP algorithm				OMP-PKS algorithm			
		First decoder method		Second decoder method		First decoder method		Second decoder method		First decoder method		Second decoder method	
NO.	*M/N*	PSNR	Time/ sec	PSNR	Time/ sec	PSNR	Time/ sec	PSNR	Time/ sec	PSNR	Time/ sec	PSNR	Time/sec
1	0.234	10.415	17.004	29.849	13.151	8.136	58.391	29.776	47.955	14.739	24.258	37.47	25.693
2	0.254	10.422	33.852	29.844	26.879	7.978	122.43	29.782	96.767	20.044	44.398	37.694	46.832
3	0.273	10.509	52.245	29.847	40.357	8.264	186.608	29.796	147.967	29.83	63.804	37.919	68.547
4	0.293	11.114	72.977	29.851	53.43	8.274	253.938	29.801	211.725	36.781	87.751	37.984	91.682
5	0.313	12.780	94.537	29.852	66.363	10.338	326.9	29.844	276.434	37.991	110.277	37.991	115.176
6	0.332	13.062	120.277	29.853	79.685	9.77	400.938	29.853	341.564	37.991	134.379	37.991	139.777
7	0.352	14.074	146.516	29.855	92.743	10.363	480.717	29.856	407.818	37.991	160.915	37.991	164.487
8	0.371	16.993	171.461	29.86	106.658	16.613	558.811	29.859	480.327	37.991	190.399	37.991	190.852
9	0.391	18.710	214.377	29.861	120.636	14.328	637.311	29.86	550.902	37.991	218.074	37.991	216.873
10	0.410	19.942	246.825	29.857	135.487	14.613	721.193	29.864	626.344	37.991	249.118	37.991	244.75
11	0.430	18.046	275.373	29.866	149.558	16.153	805.106	29.87	702.504	37.991	276.715	37.991	272.705
12	0.449	16.744	303.625	29.863	163.988	20.352	895.758	29.88	784.903	37.991	310.458	37.991	302.892
13	0.469	22.405	341.907	29.873	178.886	25.617	990.918	29.876	869.628	37.991	345.854	37.991	332.501
14	0.488	20.030	370.83	29.866	194.564	25.563	1089.059	29.881	965.038	37.991	380.096	37.991	363.763
15	0.508	24.542	403.153	29.88	210.009	29.67	1187.417	29.882	1052.617	37.991	413.075	37.991	394.776
16	0.527	26.370	434.681	29.877	225.967	29.885	1299.613	29.884	1139.416	37.991	450.094	37.991	428.036
17	0.547	25.707	476.911	29.883	241.053	29.885	1411.185	29.884	1232.424	37.991	489.921	37.991	460.624
18	0.566	26.552	506.676	29.877	258.041	29.885	1527	29.884	1335.634	37.991	530.918	37.991	496.177
19	0.586	27.588	545.442	29.883	274.281	29.885	1641.973	29.884	1435.989	37.991	572.196	37.991	530.965
20	0.605	29.175	586.938	29.884	290.926	29.885	1761.298	29.884	1533.256	37.991	612.912	37.991	568.078
21	0.625	29.496	622.631	29.883	307.384	29.885	1875.46	29.884	1631.708	37.991	656.499	37.991	604.207
22	0.645	29.272	670.477	29.884	324.654	29.885	1995.331	29.884	1734.076	37.991	699.555	37.991	643.426
23	0.664	29.463	719.913	29.883	342.812	29.885	2130.833	29.884	1837.286	37.991	742.409	37.991	682.536
24	0.684	29.082	759.257	29.884	360.628	29.885	2261.562	29.885	1946.315	37.991	794.248	37.991	723.86
25	0.703	29.670	799.458	29.884	389.035	29.885	2378.828	29.884	2053.27	37.991	842.281	37.991	764.062
26	0.723	29.697	856.633	29.885	419.44	29.885	2518.683	29.884	2168.757	37.991	891.39	37.991	807.118
27	0.742	29.885	902.076	29.885	450.656	29.885	2653.655	29.884	2279.393	37.991	940.733	37.991	849.909
28	0.762	29.885	1155.671	29.885	483.26	29.885	2792.668	29.884	2407.142	37.991	989.639	37.991	895.383
29	0.781	29.885	1385.336	29.885	515.318	29.885	2938.934	29.884	2525.032	37.991	1038.686	37.991	939.188
30	0.801	29.885	1564.846	29.885	549.061	29.885	3090.021	29.884	2652.126	37.991	1092.974	37.991	985.583
31	0.820	29.885	1694.998	29.885	583.069	29.885	3240.359	29.884	2777.551	37.991	1149.79	37.991	1031.057
32	0.840	29.885	1829.049	29.885	617.015	29.885	3350.379	29.884	2907.11	37.991	1204.187	37.991	1079.699

Table 4.2. PSNR and its execution time with different Sparsity rates *K/N* by using the three reconstruction algorithms with the first and second decoder methods.

Sparsity rates		L1-min algorithm				OMP algorithm				OMPPKS algorithm			
		First decoder method		Second decoder method		First decoder method		Second decoder method		First decoder method		Second decoder method	
NO.	*K/N*	PSNR	Time/ sec	PSNR	Time/ sec	PSNR	Time/ sec	PSNR	Time/ sec	PSNR	Time/ sec	PSNR	Time/ sec
1	21.508	27.847	30.857	29.083	23.634	32.263	109.341	30.047	94.646	33.083	52.12	33.083	23.946
2	21.992	25.696	72.338	29.219	48.828	32.817	215.422	30.185	187.607	33.219	74.381	33.219	45.303
3	22.445	25.743	111.432	29.345	72.915	32.726	319.272	30.313	280.474	33.345	99.185	33.345	66.456
4	22.988	26.857	140.604	29.494	97.625	32.65	425.337	30.457	375.182	33.494	120.573	33.494	87.875
5	23.496	27.222	192.568	29.631	122.383	32.963	531.87	30.589	480.233	33.631	142.117	33.631	109.638
6	24.137	27.129	230.226	29.803	147.577	32.149	639.62	30.753	576.548	33.803	165.174	33.803	130.994
7	24.676	26.849	272.081	29.945	171.773	32.902	743.594	30.882	675.516	33.945	187.591	33.945	152.538
8	25.352	27.195	312.236	30.121	196.374	32.484	845.135	31.054	773.203	34.121	210.711	34.121	174.269
9	26.043	27.705	351.205	30.299	221.989	32.813	951.887	31.208	872.81	34.299	233.471	34.299	195.875
10	26.789	27.524	390.814	30.49	246.809	32.986	1056.049	31.413	969.531	34.49	255.81	34.49	218.152
11	27.398	27.179	426.959	30.644	272.191	33.364	1159.181	31.569	1064.676	34.644	278.009	34.644	239.664
12	28.207	27.033	475.117	30.841	297.962	32.757	1266.323	31.748	1156.482	34.845	298.992	34.845	261.114
13	28.984	28.716	512.12	30.033	323.686	32.596	1372.076	31.931	1248.133	35.036	328.008	35.036	283.469
14	29.82	27.721	542.337	30.239	349.411	32.814	1475.567	31.123	1340.517	35.239	350.94	35.239	305.06
15	30.617	24.995	589.294	30.43	374.699	32.504	1582.1	32.307	1431.59	35.43	378.256	35.43	327.072
16	31.691	25.729	630.026	30.68	400.314	32.413	1698.289	32.547	1523.069	35.684	403.06	35.684	349.692
17	32.652	27.097	681.553	30.904	426.086	33.168	1820.594	32.758	1614.454	35.909	426.741	35.909	372.078
18	33.598	26.426	726.465	31.124	452.512	32.574	1929.28	32.97	1705.512	36.128	449.688	36.128	394.589
19	34.551	25.922	773.406	31.33	479.079	31.998	2039.089	32.162	1796.445	36.344	474.711	36.344	417.739
20	35.688	27.398	816.884	31.589	505.474	31.933	2157.665	33.383	1887.004	36.598	497.113	36.598	440.422
21	36.848	27.251	866.71	31.837	532.447	31.119	2279.112	33.641	1978.779	36.854	521.324	36.854	463.37
22	38.047	25.471	900.188	32.101	558.874	31.879	2392.728	33.853	2069.852	37.114	543.585	37.114	485.756
23	39.352	26.251	943.556	32.372	587.172	31.968	2510.633	34.11	2162.221	37.392	569.872	37.392	508.454
24	40.762	27.551	988.329	32.655	614.909	31.58	2628.196	34.358	2252.53	37.688	594.754	37.688	532.088
25	42.23	25.731	1035.285	32.973	643.582	30.951	2746.366	34.639	2344.804	38.224	619.979	38.666	554.911
26	43.887	27.703	1096.749	33.299	671.553	31.102	2866.456	34.937	2435.909	38.224	642.521	38.666	578.062
27	45.648	27.274	1150.18	33.623	700.008	30.571	2981.71	34.937	2527.107	38.224	666.701	38.666	601.54

CHAPTER 5

CONCLUSION AND SUGGESTIONS FOR FUTURE WORKS

Compressive Sensing CS is a very active area of research. It is efficient and accurate for acquiring and processing the huge data. It takes to recover the signals or the images from a few non-adaptive linear measurements. There are a different reconstruction algorithms which are used to reconstruct the sparse image such as the optimization and greedy methods.

In this thesis, we combine between the watermarking techniques and the CS theory, where the watermarking image is embedded into the measurement vectors of CS and the watermarked compressive sensing measurements resulted. The watermarked compressive sensing measurements are reconstructed by using the orthogonal matching pursuit OMP and orthogonal matching pursuit with partially known support OMP-PKS algorithms.

The OMP-PKS algorithm has a priori knowledge about some coefficients of the sparse image. All these coefficients are nonzero and considered more important than the other coefficients in the sparse signal. These nonzero coefficients are considered the partially known support PKS. The reconstructed image by the OMP and OMP-PKS consists of the original and watermarking images. Then the decoder procedure has been used to extract the watermarking image from the reconstructed watermarked CS image. The results compare the performance of the OMP and OMP-PKS algorithms. Experimental results prove that OMP-PKS algorithm improves the performance, thereby requiring a fewer samples than the OMP to reconstruct the signal.

As for the future work, we recommend to study the mathematical proof of the OMP-PKS. As well as, using the field-programmable gate array FPGA to implement this work as hardware.

REFERENCES

[1] Baraniuk, R. (2007). Compressive sensing, *IEEE signal processing magazine*, **24**.

[2] Candès, E.J. and M.B. Wakin. (2008). An introduction to compressive sampling, *Signal Processing Magazine, IEEE*, **25**, 21-30.

[3] Takeva-Velkova, V. (2010). Optimization algorithms in compressive sensing (CS) sparse magnetic resonance imaging (MRI), *MSC thesis University of Ontario Institute of Technology, June*

[4] Chen, S.S., D.L. Donoho, and M.A. Saunders. (1998). Atomic decomposition by basis pursuit, *SIAM journal on scientific computing*, **20**, 33-61.

[5] Tropp, J.A. and A.C. Gilbert. (2007). Signal recovery from random measurements via orthogonal matching pursuit, *Information Theory, IEEE Transactions on*, **53**, 4655-4666.

[6] Carrillo, R.E., L.F. Polania, and K.E. Barner. (2010). Iterative algorithms for compressed sensing with partially known support. in *Acoustics Speech and Signal Processing (ICASSP), 2010 IEEE International Conference on*, 3654-3657.

[7] Candes, E.J. and T. Tao. (2005). Decoding by linear programming, *Information Theory, IEEE Transactions on*, **51**, 4203-4215.

[8] La, C. and M.N. Do. (2006). Tree-based orthogonal matching pursuit algorithm for signal reconstruction. *In Image Processing, 2006 IEEE International Conference on*, 1277-1280.

[9] Barni, M. and F. Bartolini. (2004). Watermarking systems engineering: enabling digital assets security and other applications. CRC Press.

[10] Yamaç, M., Ç. Dikici, and B. Sankur. (2013). Robust Watermarking Of Compressive Sensed Measurements Under Impulsive And Gaussian Attacks, *In SPARS,Lausanne*.

[11] Donoho, D.L. (2006). Compressed sensing, *Information Theory, IEEE Transactions on*, **52**, 1289-1306.

[12] Garnaev, A.Y. and E.D. Gluskin. (1984). The widths of a Euclidean ball. *In Dokl. Akad. Nauk SSSR*, **277**, 1048-1052.

[13] Bourgain, J. (1989). Bounded orthogonal systems and the Λ (p)-set problem, *Acta Mathematica*, **162**, 227-245.

[14] Candes, E.J. and T. Tao. (2006). Near-optimal signal recovery from random projections: Universal encoding strategies?, *Information Theory, IEEE Transactions on*, **52**, 5406-5425.

[15] Candès, E.J., J. Romberg, and T. Tao. (2006). Robust uncertainty principles: Exact signal reconstruction from highly incomplete frequency information, *Information Theory, IEEE Transactions on*, **52**, 489-509.

[16] Donoho, D.L. (2006). High-dimensional centrally symmetric polytopes with neighborliness proportional to dimension, *Discrete & Computational Geometry*, **35**, 617-652.

[17] Donoho, D.L. (2006). For most large underdetermined systems of linear equations the minimal, *Communications on pure and applied mathematics*, **59**, 797-829.

[18] Cormode, G. and S. Muthukrishnan. (2006). Combinatorial algorithms for compressed sensing. In Structural Information and Communication Complexity. Springer.

[19] Gilbert, A.C., et al. (2002). Near-optimal sparse Fourier representations via sampling, *In Proceedings of the thiry-fourth annual ACM symposium on Theory of computing*, 152-161.

[20] Yang, F., S. Wang, and C. Deng. (2010). Compressive sensing of image reconstruction using multi-wavelet transforms. *In Intelligent Computing and Intelligent Systems (ICIS), 2010 IEEE International Conference on*, **1**, 702-705.

[21] Dias, U., M. Rane, and S. Bandewar. (2012). Survey of Compressive Sensing, *International Journal of Scientific & Engineering Research*, **3**.

[22] Wakin, M.B., et al. (2006). An architecture for compressive imaging. *In Image Processing, 2006 IEEE International Conference on*, 1273-1276.

[23] Nagesh, P. and B. Li. (2009). Compressive imaging of color images. *In Acoustics, Speech and Signal Processing, 2009. ICASSP 2009. IEEE International Conference on*, 1261-1264.

[24] Piccardi, M. (2004). Background subtraction techniques: a review. *In Systems, man and cybernetics, 2004 IEEE international conference on*, **4**, 3099-3104.

[25] Chan, W.L., et al. (2008). A single-pixel terahertz imaging system based on compressed sensing, *Applied Physics Letters*, **93**, 121105.

[26] Jung, H., et al. (2009). k-t FOCUSS: A general compressed sensing framework for high resolution dynamic MRI, *Magnetic Resonance in Medicine*, **61**, 103-116.

[27] Herrmann, F.J. and G. Hennenfent. (2008). Non-parametric seismic data recovery with curvelet frames, *Geophysical Journal International*, **173**, 233-248.

[28] Hennenfent, G. and F.J. Herrmann. (2008). Simply denoise: wavefield reconstruction via jittered undersampling, *Geophysics*, **73**, V19-V28.

[29] Du, D. and F. Hwang. (1993). Combinatorial group testing and its applications. World Scientific.

[30] Mohtashemi, M., et al. (2010). Sparse sensing DNA microarray-based biosensor: Is it feasible? *In Sensors Applications Symposium (SAS), 2010 IEEE*, 127-130.

[31] Baraniuk, R. and P. Steeghs. (2007). Compressive radar imaging. *In Radar Conference, 2007 IEEE*, 128-133.

[32] Herman, M.A. and T. Strohmer. (2009). High-resolution radar via compressed sensing, *Signal Processing, IEEE Transactions on*, **57**, 2275-2284.

[33] Moses, R.L., L.C. Potter, and M. Cetin. (2004). Wide-angle SAR imaging. *In Defense and Security*, 164-175.

[34] Qu, L. and T. Yang. (2012). Investigation of air/ground reflection and antenna beamwidth for compressive sensing SFCW GPR migration imaging, *Geoscience and Remote Sensing, IEEE Transactions on*, **50**, 3143-3149.

[35] Walden, R.H. (1999). Analog-to-digital converter survey and analysis, *IEEE Journal on selected areas in communications*, **17**, 539-550.

[36] Laska, J.N., et al. (2007). Theory and implementation of an analog-to-information converter using random demodulation. *In Circuits and Systems, 2007. ISCAS 2007. IEEE International Symposium on*, 1959-1962.

[37] Kirolos, S., et al. (2006). Analog-to-information conversion via random demodulation. *In Design, Applications, Integration and Software, 2006 IEEE Dallas/CAS Workshop on*, 71-74.

[38] Tropp, J.A., et al. (2006). Random filters for compressive sampling and reconstruction. *In Acoustics, Speech and Signal Processing, 2006. ICASSP 2006 Proceedings. 2006 IEEE International Conference on*, **3**, III-III.

[39] Mishali, M. and Y.C. Eldar. (2010). From theory to practice: Sub-Nyquist sampling of sparse wideband analog signals, *Selected Topics in Signal Processing, IEEE Journal of*, **4**, 375-391.

[40] Donoho, D.L. and B.F. Logan. (1992). Signal recovery and the large sieve, *SIAM Journal on Applied Mathematics*, **52**, 577-591.

[41] Tibshirani, R. (1996). Regression shrinkage and selection via the lasso, *Journal of the Royal Statistical Society. Series B (Methodological)*, 267-288.

[42] Donoho, D.L. (1995). De-noising by soft-thresholding, *Information Theory, IEEE Transactions on*, **41**, 613-627.

[43] O'Brien, M.S., A.N. Sinclair, and S.M. Kramer. (1994). Recovery of a sparse spike time series by l 1 norm deconvolution, *Signal Processing, IEEE Transactions on*, **42**, 3353-3365.

[44] Candes, E.J., J.K. Romberg, and T. Tao. (2006). Stable signal recovery from incomplete and inaccurate measurements, *Communications on pure and applied mathematics*, **59**, 1207-1223.

[45] Needell, D. and R. Vershynin. (2010). Signal recovery from incomplete and inaccurate measurements via regularized orthogonal matching pursuit, *Selected Topics in Signal Processing, IEEE Journal of*, **4**, 310-316.

[46] Donoho, D.L. and M. Elad. (2003). Optimally sparse representation in general (nonorthogonal) dictionaries via ℓ1 minimization, *Proceedings of the National Academy of Sciences*, **100**, 2197-2202.

[47] Donoho, D. and J. Tanner. (2009). Counting faces of randomly projected polytopes when the projection radically lowers dimension, *Journal of the American Mathematical Society*, **22**, 1-53.

[48] Fuchs, J.-J. (2004). On sparse representations in arbitrary redundant bases, *Information Theory, IEEE Transactions on*, **50**, 1341-1344.

[49] Natarajan, B.K. (1995). Sparse approximate solutions to linear systems, *SIAM journal on computing*, **24**, 227-234.

[50] Gribonval, R., et al. (1996). Analysis of sound signals with high resolution matching pursuit. *In Time-Frequency and Time-Scale Analysis, 1996., Proceedings of the IEEE-SP International Symposium on*, 125-128.

[51] Banham, M.R. and J.C. Brailean. (1997). A selective update approach to matching pursuits video coding, *Circuits and Systems for Video Technology, IEEE Transactions on*, **7**, 119-129.

[52] Hastie, T., et al. (2009). The elements of statistical learning. 2: Springer.

[53] Rath, G. and C. Guillemot. (2009). Sparse approximation with an orthogonal complementary matching pursuit algorithm. *In Acoustics, Speech and Signal Processing, 2009. ICASSP 2009. IEEE International Conference on*, 3325-3328.

[54] Wang, J., S. Kwon, and B. Shim. (2012). Generalized orthogonal matching pursuit, *Signal Processing, IEEE Transactions on*, **60**, 6202-6216.

[55] Donoho, D.L., et al. (2012). Sparse solution of underdetermined systems of linear equations by stagewise orthogonal matching pursuit, *Information Theory, IEEE Transactions on*, **58**, 1094-1121.

[56] Needell, D., J. Tropp, and R. Vershynin. (2008). Greedy signal recovery review. *In Signals, Systems and Computers, 2008 42nd Asilomar Conference on*, 1048-1050.

[57] Rebollo-Neira, L. (2001). Frames in two dimensions arising from wavelet transforms, *Proceedings of the Royal Society of London. Series A: Mathematical, Physical and Engineering Sciences*, **457**, 2079-2091.

[58] Mallat, S.G. and Z. Zhang. (1993). Matching pursuits with time-frequency dictionaries, *Signal Processing, IEEE Transactions on*, **41**, 3397-3415.

[59] Rebollo-Neira, L. and D. Lowe. (2002). Optimized orthogonal matching pursuit approach, *Signal Processing Letters, IEEE*, **9**, 137-140.

[60] Needell, D. and J.A. Tropp. (2009). CoSaMP: Iterative signal recovery from incomplete and inaccurate samples, *Applied and Computational Harmonic Analysis*, **26**, 301-321.

[61] Jacques, L. (2010). A short note on compressed sensing with partially known signal support, *Signal Processing*, **90**, 3308-3312.

[62] Vaswani, N. and W. Lu. (2010). Modified-CS: Modifying compressive sensing for problems with partially known support, *Signal Processing, IEEE Transactions on*, **58**, 4595-4607.

[63] Duarte, M.F., et al. (2009). Recovery of compressible signals in unions of subspaces. *In Information Sciences and Systems, 2009. CISS 2009. 43rd Annual Conference on*, 175-180.

[64] Sermwuthisarn, P., et al. (2012). Impulsive noise rejection method for compressed measurement signal in compressed sensing, *EURASIP Journal on Advances in Signal Processing*, **2012**, 1-23.

[65] Sermwuthisarn, P., et al. (2012). Robust reconstruction algorithm for compressed sensing in Gaussian noise environment using orthogonal matching pursuit with partially known support and random subsampling, *EURASIP Journal on Advances in Signal Processing*, **2012**, 1-21.

[66] Cevher, V., et al. (2008). Compressive sensing for background subtraction. In Computer Vision–ECCV 2008. Springer.

[67] Cox, I.J. and M.L. Miller. (2002). The first 50 years of electronic watermarking, *EURASIP Journal on Applied Signal Processing*, **2002**, 126-132.

[68] Swanson, M.D., B. Zhu, and A.H. Tewfik. (1996). Robust data hiding for images. *In Digital Signal Processing Workshop Proceedings, 1996., IEEE*, 37-40.

[69] Hernandez, J.R., M. Amado, and F. Perez-Gonzalez. (2000). DCT-domain watermarking techniques for still images: Detector performance analysis and a new structure, *Image Processing, IEEE Transactions on*, **9**, 55-68.

[70] Hartung, F. and B. Girod. (1998). Watermarking of uncompressed and compressed video, *Signal processing*, **66**, 283-301.

[71] http://www.geovision.com.tw.

[72] http://www.mediasec.com.

[73] Kirstein, M., *Beyond traditional DRM: Moving to digital watermarking and fingerprinting in media monetization*. 2006, January.

[74] Huang, H.-C., et al. (2012). Watermarking for compressive sampling applications. *In Intelligent Information Hiding and Multimedia Signal Processing (IIH-MSP), 2012 Eighth International Conference on*, 223-226.

[75] Huang, H.-C., et al. (2011). Tabu search based multi-watermarks embedding algorithm with multiple description coding, *Information Sciences*, **181**, 3379-3396.

[76] Kundur, D. and D. Hatzinakos. (1997). A robust digital image watermarking method using wavelet-based fusion. *In International Conference on Image Processing*, **3**, 544-547.

[77] Orovic, I. and S. Stankovic. (2013). Combined compressive sampling and image watermarking. *In ELMAR, 2013 55th International Symposium*, 41-44.

[78] Orović, I., A. Draganić, and S. Stanković. (2013). Compressive Sensing as a Watermarking Attack, 21st Telecommunications Forum TELFOR 2013, Novembar.

[79] Simmons, G.J. (1984). The prisoners' problem and the subliminal channel. *In Advances in Cryptology*, 51-67.

[80] Qaisar, S., et al. (2013). Compressive sensing: From theory to applications, a survey, *Communications and Networks, Journal of*, **15**, 443-456.

[81] Tiesheng, F., et al. (2013). A Digital Image Watermarking Method Based on the Theory of Compressed Sensing, *International Journal of Automation and Control Engineering*, **2**.

[82] M. Yamac, C. Dikici, and B. Sankur. (2013). Watermarking of Compressive Sensed Measurements, *in SPARS,Lausanne*.